Università degli Studi di Palermo

AREA QUALITÀ, PROGRAMMAZIONE E SUPPORTO STRATEGICO
SETTORE STRATEGIA PER LA RICERCA U. O. DOTTORATI

Dottorato di ricerca in Biomedicina e Neuroscienze
Dipartimento in Biomedicina, Neuroscienze e Diagnostica avanzata (BI.N.D.)

SSD BIO/16

Cancer-related cachexia: insight for a multimodal approach

IL DOTTORE

GIUSEPPE DONATO MANGANO

IL COORDINATORE

Chiar.mo Prof. **FABIO BUCCHIERI**

IL TUTOR

Chiar.mo Prof. **ROSARIO BARONE**

CICLO XXXV
ANNO CONSEGUIMENTO TITOLO 2023

List of contents

Introduction

Cachexia is a common complication in cancer patients, characterized by involuntary weight loss and reduction in muscle mass, often associated with a general feeling of weakness and fatigue. Cancer-related cachexia is frequently a complication of advanced cancer, but it may also be present in the early stages of the disease. Cachexia is associated with increased morbidity and mortality in cancer patients, with a reduction in the effectiveness of anti-tumor therapy, and a worsening of quality of life. Cancer-related cachexia is a complex syndrome including different pathological processes all driven by the single underlying tumor cause. Therefore, the only decisive intervention for this syndrome would be the elimination of the tumor. Since various clinical conditions, do not always allow an effective treatment of the tumor, to day, in line with the increasing focus on the quality of life of cancer patients, treating the most disabling symptoms remains the only feasibletherapeutic option. Furthermore, even well-established therapeutic protocols, such as chemotherapy or radiotherapy, often cause side effects that reduce their effectiveness. Therefore, the development of multimodal approaches, both pharmacological and non-pharmacological, become the main challenge in the field of oncology.

In particular, the development of a therapeutic model that takes effectdirectly on the tumor and simultaneously restores the general homeostasis of the organism seems to give relevant advantages, including a reduction in drugs resistance, increasing in their effectiveness, and the protection of organs from the non-selective action of chemotherapeutic agents.Of course, tumor excision remains the main goal, but a comprehensive approach that also addresses the broader systemic effects of cancer-related cachexia could improve the overall well-being of cancer patients and lead to better treatment outcomes. Therefore, understanding the pathogenetic mechanisms underlying cachexia is a relevant research area that could lead to the development of targeted therapies to improve cancer patient care.

Based on the above considerations, the present project consists of two studies. The first study investigated the effect of physical exercise on both tumor and skeletal muscles of cachectic mice, with a focus on identifying potential therapeutic targets such as Hsp60

and Pgc1-alpha.The aim was to achieve a better understanding of the role that physical activity can play in cachexia in cancer patients.

The second study aimed to refine the use of cisplatin chemotherapy in tumor-bearing mice by identifying the lowest effective dose that minimizes side effects. This is an important step in planning new therapeutic protocols that can improve the effectiveness of chemotherapy while reducing its negative impact on patients' quality of life. The findings of these studies could have relevant implications for the treatment of cancer-related cachexia, as well as for the development of new therapeutical drugs.

Abstract

Study 1: The effect of exercise training on C26 tumor-bearing mice

Cancer-related cachexia is a syndrome that affects multiple organs and is mainly characterized by an involuntary loss of muscle mass and changes in adipose tissue. Recently, significant advances in our understanding of cachexia's underlying mechanism highlighted the role of inflammatory cytokines signalling in driving abnormal cross-talk between different tissues leading to a structural and metabolic shift in skeletal muscle. In this context, physical exercise has long been recognized as having relevant health benefits, including the ability to restore whole-body homeostasis through the modulation of anabolic and catabolic stimuli. In line with these findings, the present study was designed to compare the effects of different training protocols on various aspects of cachexia, including lifespan, tumor growth, onset of cachexia, and skeletal muscle homeostasis.

The experiments were carried out on one hundred and fifty 3-month-old male BALB/c mice divided into six groups in relation to the tumor inoculum and the exercise training protocols that were administered (i.e., sedentary/inoculated/sedentary=SED/I/SED; sedentary/inoculated/training progressive=SED/I/TR_P; training progressive/inoculated/training low intensity=TR_P/I/TR_L; training

progressive/inoculated/training high intensity=$TR_P/I/TR_H$; sedentary/training=SED/TR, and sedentary/sedentary=SED/SED). Clinical parameters including lifespan, tumor growth, and the onset of cachexia were evaluated. At the molecular level, we studied Hsp60, Isolectin, and Pgc1α proteins expression as a marker of oxidative stress, vascularization, and mitochondrial biogenesis, respectively.

The results showed a significant increase in the lifespan's average of the $TR_P/I/TR_H$ group compared to the other groups and a significant difference between the $TR_P/I/TR_H$ and the $SED/I/TR_P$ in cachexia onset. Further, exercise training modulated the pro-inflammatory cytokines pattern reducing IL-1, IL-6 and TNFα released from the tumor and it interfered with the tumor growth increasing the apoptosis process while inhibiting the cellular proliferation. The immunofluorescences analysis showed increased immunoreactivity of Hsp60 in tumor and skeletal muscles (in particular in soleus muscle compared to plantaris and gastrocnemius muscles) of the trained groups compared with the sedentary counterparts. Immunoreactivity of Isolectin was significantly increased in white gastrocnemius and soleus muscles from $SED/I/TR_P$ and $TR_P/I/TR_H$ groups compared to the not-bearing tumor groups. In plantaris and red gastrocnemius muscles from $TR_P/I/TR_H$ group was found a higher level of Isolectin compared to the SED/SED group, while the amount of this protein was significantly increased in the $SED/I/TR_P$ group compared to both SED/SED and SED/TR groups in the same muscles. Immunofluorescence analysis for Pgc1α showed high protein levels in soleus, plantaris, and red gastrocnemius muscles from $SED/I/TR_P$ and $TR_P/I/TR_H$ groups compared with the SED/SED group.

Overall these findings suggest a promising role of physical exercise in improving life quality in chronic diseases such as cancer-related cachexia. Therefore, knowledge about the molecular pathways underlying the healthful effects of physical exercise could represent a crucial issue to develop a new therapeutic target.

Introduction

Cachexia is a multifactorial syndrome that can be caused by various underlying medical conditions, such as cancer, chronic obstructive pulmonary disease, heart failure, and HIV/AIDS. It is characterized by progressive muscle wasting, loss of body weight, and reduced physical function and quality of life. Cachexia is associated with poor clinical outcomes, including increased morbidity and mortality, and decreased response to treatments. Therefore, it is important to diagnose and manage cachexia promptly and effectively (Von Haehling, S.&Anker, S.D. 2010).

The diagnosis of cachexia is based on several criteria, including weight loss greater than 5% in the past six months or less than 20% of the ideal body weight, and the presence of at least three of the following: decreased muscle strength, fatigue, anorexia, low fat-free mass index, and abnormal biochemistry (e.g., increased inflammatory markers, anemia, and hypoalbuminemia) (Fearon et al., 2011). In addition, imaging studies such as computed tomography (CT) scans can be used to assess the extent of muscle wasting and fat loss.

The pathophysiology of cachexia is complex and not fully understood, but it is thought to involve a combination of systemic inflammation, altered metabolism, and neuroendocrine dysfunction (Baracos et al., 2018). In particular, elevated levels of pro-inflammatory cytokines, such as tumor necrosis factor-alpha (TNF-α), interleukin-6 (IL-6), and interleukin-1 beta (IL-1β), are associated with muscle wasting and increased metabolic rate, leading to weight loss and fatigue (Dev et al., 2015). Moreover, the loss of appetite and anorexia associated with cachexia are linked to dysregulation of the hypothalamus-pituitary-adrenal (HPA) axis, resulting in impaired food intake and metabolism (Evans et al., 2008).

The treatment of cachexia is complex and often requires a multimodal approach that addresses the underlying disease, promotes adequate nutrition and physical activity, and takes into account the inflammatory and metabolic pathways involved in the development of cachexia. Current treatment options include nutritional support, exercise training, pharmacological interventions (e.g., corticosteroids, nonsteroidal anti-inflammatory drugs), and supportive care (e.g., pain management, psychological

support) (Sadeghi et al., 2018; Solheim et al., 2018). However, the effectiveness of these interventions is poor, and more research is needed to better understand the underlying pathophysiology of cachexia.

Cancer-related Cachexia

Cancer-related cachexia is a complex metabolic syndrome that affects up to 80% of patients with advanced cancer. (Arends et al., 2021). It is characterized by the loss of skeletal muscle mass and strength, as well as anorexia, fatigue, and weight loss. This condition has been associated with poor quality of life, increased morbidity, and mortality (Schmidt SF. et al., 2018).

The pathophysiology of cancer cachexia is multifactorial, involving a complex interplay of systemic inflammation, dysregulated protein metabolism, and altered lipid metabolism, among other factors (Peixoto da Silva et al., 2020). It has also been linked to cancer-related pain, which may exacerbate cachexia symptoms (Law ML. 2022).

Cancer cachexia affects multiple organs, such as the liver, the heart, and the lungs, which contribute to the metabolic alterations seen in cachexia (Siddiqui et al., 2020). Animal studies helped to identify key phenotypic features of cancer cachexia, such as impaired mitochondrial function and increased oxidative stress (Brown et al., 2020; Martin & Freyssenet, 2021). Patients with cancer cachexia experience important impacts on their health-related quality of life across all stages of the condition. The symptoms can be profound, including physical changes such as muscle wasting and fatigue, as well as emotional changes such as depression and anxiety (Kasvis et al., 2019).

Current therapeutic interventions for cancer cachexia include nutritional support, exercise, and pharmacological treatments aimed at targeting the underlying metabolic dysfunction (Fonseca et al., 2020; Siddiqui et al., 2020). Nutritional support may involve a combination of oral, enteral, or parenteral feeding, depending on the patient's needs and tolerance. Exercise interventions may include resistance training and aerobic exercise, while pharmacological treatments may involve the use of appetite stimulants, anti-inflammatory drugs, and anabolic agents.

In summary, cancer cachexia is a multifactorial syndrome that involves systemic inflammation, dysregulated protein and lipid metabolism and impacts multiple organs in the body. It greatly affects the quality life of patients and is associated with poor prognosis. Treatment approaches include nutritional support, exercise, and pharmacological interventions, aimed at addressing the underlying metabolic dysfunction.

Exercise training and cancer

An interesting review highlighted that the traditional dogma recommending rest and inactivity to cancer patients changed over the past two decades (Christensen et al. 2018). The Authors argued that exercise had multiple benefits in patients with cancer, including a decrease of treatment-related side effects, improved quality of life, and potentially decreased risk of recurrence and mortality. However, the type of exercise and its intensity should be chosen carefully, depending on the patient's condition and individual preferences, taking into account factors such as the stage of cancer, comorbidities, and any physical limitations.

It has been reported that both endurance training and resistance training can be effective in improving physical function, reducing fatigue, and enhancing the quality of life in cancer patients (Mok J. et al., 2022). Endurance training, such as walking, cycling, and swimming, has been found to improve cardiorespiratory fitness, oxygen uptake, and metabolic function in cancer patients with impaired physical function due to cancer and its treatments (Kneis S. et al., 2019). Resistance training, such as weightlifting, can help to increase muscle mass and strength, improve bone density, and reduce the risk of falls and fractures, which can be particularly important for older cancer patients (Shailendra P. et al., 2022). The molecular mechanisms underlying the healthy effects of exercise on cancer are complex and multifactorial. Exercise is known to activate multiple signaling pathways that can promote DNA repair, reduce inflammation, and modulate cellular metabolism. One of the key pathways activated by exercise is the AMP-activated protein kinase (AMPK) pathway, which plays a critical role in regulating energy metabolism and cellular stress responses. Exercise-induced activation of AMPK can

increase glucose uptake and fatty acid oxidation, leading to enhanced mitochondrial function and decreased oxidative stress, which in turn can reduce the risk of cancer development and progression (Hojman P. et al., 2018).

A recent study conducted on C2C12 myotubes and mice has discovered a fascinating correlation between the availability of free fatty acids and IL-13 signalling. Surprisingly, IL-13 does not seem to cause any significant changes in metabolic gene expression in normal physiological conditions, nor in mice deficient in IL-13 at rest. However, during intense exercise and endurance training, IL-13 signalling appears to be crucial, as demonstrated by reduced utilization of fatty acids and impaired mitochondrial biogenesis in mice deficient in IL-13. Moreover, increased mitochondrial respiration, endurance performance, and glucose tolerance were observed in mice when IL-13/IL-13Ra1 binding occurred, which led to downstream activation of STAT3 signalling. Both IL-13 treatment in C2C12 myotubes and exercise training in mice resulted in increased levels of phosphorylation of STAT3 (Knudsen NH. Et al., 2020).

Exercise can also reduce the production of pro-inflammatory cytokines and chemokines, which can contribute to the development and progression of cancer. Several studies have highlighted the anti-inflammatory benefits of physical exercise (Bordignon C. et al., 2022). In particular, a combination of aerobic and resistance training in cancer survivors has been found to reduce TNF-α and C-reactive protein levels while increasing the production of anti-inflammatory cytokines, such as IL-10 and IL-1ra, which may help mitigate the harmful effects of chronic inflammation (Khosravi N. et al ., 2019).

In tumor-bearing rats resistance exercise training increased the IL-10/TNF-α ratio and circulating IL-10 levels mitigating tumor-induced systemic pro-inflammatory conditions (Padilha CS et al., 2017). Interestingly, it has been reported that Interleukin-6 (IL-6) is a multifunctional cytokine playing an important role in the immune system and inflammatory response. Moreover, IL-6 has been shown to be involved in the organism's adaptation to exercise and in the pathogenesis of many diseases, including cancer (Uciechowski P & Dempke WCM. 2020)). In the context of exercise, IL-6 is secreted by skeletal muscles during resistance and aerobic exercise, and this secretion

can be increased by exercise-induced muscle inflammation (Steensberg A. et al 2002). Unlike the controversial role of IL-6 in cancer pathogenesis, studies suggest that exercise may have a beneficial effect on cancer patients by reducing systemic inflammation and regulating IL-6. In particular, exercise seems to have an anti-inflammatory effect that can reduce circulating IL-6 levels in cancer cachexia patients (Petersen AM. & Pedersen BK. 2006). Moreover, exercise appears to increase IL-6 production at the muscle level, promoting a local anti-inflammatory response (Daou HN. Et al., 2020). Another important mechanism by which exercise can prevent and treat cancer is by modulating the immune system. In particular, by increasing the production and circulation of immune cells such as natural killer (NK) cells, T cells, and B cells, it can eliminate cancer cells and prevent the formation of new tumors (Khosravi N. et al., 2019). Moreover, exercise can also modulate the expression and activity of various growth factors and hormones as well as tumor suppressor genes and oncogenes affecting cancer cell growth and proliferation (Hojman P. et al., 2018). In conclusion, physical exercise represents an important non-pharmacological strategy in the management of cancer patients, as it can improve quality of life, reduce systemic inflammation, and modulate the production of growth factors and hormones that can influence the growth of tumor cells.

Heat shock proteins

Heat shock proteins (HSPs) are a family of highly conserved proteins that are expressed in response to a variety of cellular stresses, including heat shock, oxidative stress, and inflammation. The structure of HSPs is characterized by a conserved domain, known as the heat shock domain (HSD), which facilitates their ability to bind to misfolded or denatured proteins and prevent their aggregation (Bukau B. et al., 2006). HSPs are classified into five major families based on their molecular weight (HSP40, HSP60, HSP70, HSP90, HSP100), of which the most well-known are the Hsp70 and Hsp90 families (Jee H. et al., 2016).

The primary function of HSPs is the protection of cells from damage caused by stress by promoting the refolding or degradation of misfolded proteins, preventing protein

aggregation, and maintaining cellular homeostasis. In addition to their cytoprotective functions, HSPs are also involved in a range of cellular processes, including protein trafficking, signal transduction, and gene expression (Hartl FU & Hayer-Hartl M. 2002). HSPs have been implicated in a variety of human diseases, including cancer, neurodegenerative disorders, and cardiovascular disease, highlighting their importance in maintaining cellular health (Macario AJ, Conway de Macario E. 2007).

The expression and activity of HSPs are tightly regulated by a complex network of signalling pathways, including the heat shock response (HSR) and other stress response pathways. The HSR is initiated by the activation of heat shock factor 1 (HSF1), which binds to heat shock elements (HSEs) in the promoter region of HSP genes, leading to the upregulation of HSP expression. Other stress response pathways, such as the unfolded protein response (UPR) and the oxidative stress response, also contribute to the regulation of HSP expression and activity (Hagymasi AT. Et al., 2022; Akerfelt M. et al., 2010).

Overall, the structure, function, and regulation of HSPs are critical for maintaining cellular homeostasis and protecting cells from damage caused by stress. The understanding of HSPs and their role in cellular stress response continues to advance, with potential implications for the development of novel therapeutic strategies for a range of human diseases.

Heat shock protein 60

Heat shock protein 60, also known as Hsp60, is a chaperonin present in all living organisms, from bacteria to humans (Gupta RS. 1995). This protein is involved in several cellular processes, including protein synthesis, DNA repair, and regulation of cellular metabolism. Hsp60 acts as a chaperonin protein, which assists other proteins in correctly folding and assuming their correct three-dimensional conformation. Moreover, recent studies have shown that Hsp60 undergoes several post-translational modifications, such as phosphorylation, acetylation, and methylation, which can influence its function and have pathological consequences (Caruso Bavisotto C. et al., 2020). For instance, phosphorylated Hsp60 may be involved in the progression of

certain diseases, such as cancer and neurodegenerative diseases. Recent studies have shown that Hsp60 can also regulate the activity of immune cells, such as T cells and dendritic cells, through its interaction with toll-like receptors (TLRs) (Cappello F. et al., 2014). Hsp60 can activate TLRs, leading to the production of cytokines and chemokines, which are important for the recruitment and activation of immune cells. Additionally, Hsp60 can directly interact with T cells, promoting their differentiation into regulatory T cells, which play a crucial role in maintaining immune tolerance and preventing autoimmunity. This can have important implications for the development of vaccines and immune therapies that use antigens presented by Hsp60. In general, the involvement of Hsp60 in the immune response of the body highlights its key role in the pathogenesis of many human diseases and its potential utility as a therapeutic target or diagnostic biomarker.

Hsp60 has been studied in relation to colorectal cancer (CRC), one of the leading causes of cancer-related deaths worldwide. In this context, Hsp60 has been found to be overexpressed in CRC tissues compared to normal colon tissues. Furthermore, Hsp60 has been shown to interact with several molecules involved in the regulation of cell proliferation and apoptosis, such as Bax and Bcl-2, suggesting a possible role in CRC pathogenesis (Cappello F., et al., 2011). Hsp60 has also been proposed as a potential diagnostic and therapeutic target for CRC, as its levels have been found to be significantly higher in the serum of CRC patients compared to healthy controls, and as several Hsp60 inhibitors have shown promising results in preclinical studies. Therefore, understanding the molecular anatomy and role of Hsp60 in CRC may provide important insights into the development of novel diagnostic and therapeutic approaches for this deadly disease.

On one hand, Hsp60 is overexpressed in various types of cancer cells and plays a crucial role in cancer cell survival and proliferation. Therefore, inhibition of Hsp60 could potentially induce cancer cell death and inhibit tumor growth. On the other hand, Hsp60 is also expressed in normal cells and plays important roles in cellular homeostasis and function. Therefore, Hsp60-targeted therapies could have potential side effects such as disruption of normal cellular processes and induction of inflammation (Cappello F. et al., 2013).

According to Marino Gammazza et al., Hsp60 plays a crucial role in skeletal muscle fiber biogenesis and homeostasis. The protein helps to maintain the integrity of mitochondria and facilitates the formation of new muscle fibers. It also regulates muscle protein synthesis and degradation, and helps to prevent muscle damage caused by oxidative stress (Marino Gammazza A. et al., 2018). Hsp60 expression seems to be increased in response to chronic physical exercise showing a fiber specificity expression in type I and IIa muscle fibers although there isn't accordance in the scientific community (D'Amico D. et al., 2021; Folkesson M. et al., 2013; Morton JP. Et al., 2008). These findings highlight the important role of Hsp60 in skeletal muscle biology and suggest its potential as a therapeutic target for muscle disorders.

Pgc1 alpha

Peroxisome proliferator-activated receptor gamma coactivator 1-alpha (PGC-1α) is a transcriptional coactivator that plays a key role in the regulation of cellular energy metabolism and adaptation to various stress stimuli. PGC-1α was originally identified as a coactivator of PPARγ, a nuclear receptor involved in adipocyte differentiation and glucose metabolism (Muoio DM. et al., 2007). It is expressed in a wide range of tissues, including skeletal muscle, heart, liver, and brain, and is subject to extensive post-translational modifications, including phosphorylation, acetylation, and ubiquitination, which can modulate its activity and stability (Rius-Pérez S. et al., 2020). PGC-1α is also subject to alternative splicing, which generates several isoforms that differ in their N- and C-terminal regions and in their ability to interact with other transcriptional regulators. The various isoforms of PGC-1α have been shown to have distinct functions in different tissues and under different physiological conditions. For example, PGC-1α4, a muscle-specific isoform, has been shown to promote mitochondrial biogenesis and oxidative metabolism in skeletal muscle, while PGC-1α1, the most widely expressed isoform, has been implicated in the regulation of hepatic gluconeogenesis and thermogenesis in brown adipose tissue (Martínez-Redondo V. et al., 2015).

Silvennoinen et al. investigated the expression of different isoforms of Pgc1-alpha in human skeletal muscle following resistance and endurance exercise. They found that the expression of Pgc1-alpha isoforms varied between the two types of exercise. Specifically, the Pgc1-alpha4 isoform was upregulated after resistance exercise, while Pgc1-alpha1 and Pgc1-alpha3 were upregulated after endurance exercise. Additionally, the authors observed that different target genes were activated by these isoforms, with Pgc1-alpha4 primarily regulating genes involved in muscle growth and Pgc1-alpha1 and Pgc1-alpha3 regulating genes involved in mitochondrial biogenesis and oxidative metabolism (Silvennoinen M. et al., 2015). These findings suggest that the expression of Pgc1-alpha isoforms may play a key role in mediating the adaptations to different types of exercise, highlighting the importance of tailoring training programs to individual goals and needs. Moreover, in a recent pilot study, D'Amico and colleagues investigated the expression of different PGC-1α isoforms in male and female skeletal muscle following a single bout of exercise. The researchers found that male participants exhibited a significant increase in PGC-1α1 and PGC-1α4 isoforms, while female participants only showed a significant increase in PGC-1α4. The PGC-1α4 isoform is known to be involved in mitochondrial biogenesis and muscle fiber type switching, suggesting that females may have a greater potential for these adaptations compared to males. The study also found that there were no sex-based differences in the expression of PGC-1α2 and PGC-1α3 isoforms (D'Amico D. et al., 2021). The findings of this study suggest that there may be sex-based differences in the expression of PGC-1α isoforms in skeletal muscle following exercise, which could have important implications for designing exercise programs that are optimized for each gender.

Another interesting study investigates the role of the transcriptional co-activator PGC-1 alpha in driving the formation of slow-twitch muscle fibers (Lin J. et al., 2002). Slow-twitch muscle fibers are important for endurance activities, such as long-distance running, and are characterized by their high oxidative capacity and fatigue resistance. The researchers used transgenic mice with muscle-specific overexpression of PGC-1 alpha to examine its effects on muscle fiber type composition. They found that PGC-1 alpha was sufficient to induce a shift towards a greater proportion of slow-twitch fibers, as evidenced by increased expression of genes associated with oxidative metabolism and slow-twitch fiber type. Additionally, the mice with PGC-1 alpha overexpression

showed improved endurance exercise performance compared to control mice. Futher, Baar showed that Pgc1-alpha co-activates the peroxisome proliferator-activated receptor gamma (PPARγ), nuclear respiratory factors (NRF1 and NRF2), and PPARα, leading to the transcriptional activation of genes involved in mitochondrial biogenesis, fatty acid oxidation, and angiogenesis. Additionally, Pgc1-alpha has been shown to interact with other transcription factors, such as myocyte enhancer factor 2 (MEF2) and estrogen-related receptor alpha (ERRα), to further enhance mitochondrial biogenesis and oxidative metabolism in response to endurance exercise (Baar K. 2004).

Beside its role in healthy conditions, PGC-1α has been shown to play a significant role in promoting tumor growth and survival by facilitating angiogenesis, DNA repair, and modulating immune cell activity (Bost F, Kaminski L. 2019). One of the key mechanisms by which PGC-1α promotes angiogenesis is by upregulating the expression of vascular endothelial growth factor (VEGF), a potent stimulator of blood vessel growth (Igarashi J. et al., 2016). PGC-1α has also been found to facilitate DNA repair through its ability to activate the base excision repair pathway, which repairs oxidative DNA damage. Additionally, PGC-1α modulates immune cell activity by promoting the differentiation of regulatory T cells and M2 macrophages, both of which have been shown to play a role in promoting tumor growth and survival(Boutilier AJ, Elsawa SF. 2021).

Furthermore, PGC-1α is also known to increase the expression of glucose transporters, such as GLUT1 and GLUT3, which in turn enhance glucose uptake and metabolism in cancer cells (Zhang HL. Et al., 2017). Additionally, PGC-1α can increase the expression of antioxidant enzymes, including superoxide dismutase (SOD) and catalase, which protect cancer cells from damage caused by oxidative stress. These mechanisms contribute to an increased supply of energy and adaptation to the altered nutrient and oxygen availability in the tumor microenvironment, thereby promoting the survival and growth of cancer cells (Rius-Pérez S. et al., 2020).

Hence, a more comprehensive understanding of the complex molecular mechanisms mediated by PGC-1α in both normal and cancerous cells is essential for the development of innovative therapeutic approaches that aim to prevent or oppose cancer.

Research Aims

The present study investigated the effect of physical exercise on both tumor and skeletal muscles of cachectic mice, with a focus on identifying potential therapeutic targets such as Hsp60 and Pgc1-alpha. The aim was to gain a better understanding of the role of physical activity in counteracting cachexia in cancer patients.

Materials and Methods

Animals

This experiment was carried out on one hundred and fourty six 3-month-old male mice (BALB/c AnNHsd), obtained from Harlan Laboratories S.r.l. (Udine, Italy). All mice were maintained at a constant temperature of 21 ± 2 °C with controlled lighting (12-hrs light-dark cycle) and were allowed free access to food and water. Four mice were inoculated with a frozen fragment of solid C26 tumor (C26 tumor-bearing mice) using a trocar and after were used as a donor of a fresh fragment of C26 tumor. These animals were euthanized by cervical dislocation, after that tumor mass was dissected and a fragment of colon carcinoma (0.3 mm3) was subcutaneously inoculated in the left flank of the experimental mice. Particular attention was pointed to the selection of the fresh fragment of C26 inoculated, the fragment presented a pretty solid consistency and necrotic areas and the capsule around the tumor were carefully discarded. Part of the tumors of tumor-bearing mice was fixed in formalin for further analyses.

All animal experiments were approved by the Committee on the Ethics of Animal Experiments of the University of Palermo and adhered to the recommendations in the Guide for the Care and Use of Laboratory Animals by the USA National Institute of Health (NIH). All experiments were performed in the Human Physiology Laboratory of the Department of Experimental Biomedicine and Clinical Neurosciences of the

University of Palermo, which was formally authorized by the Italian Ministry of Health (Roma, Italy).

Experimental design

One hundred mice were used for the survival study and they were divided into four groups: sedentary/inoculated/sedentary=SED/I/SED; sedentary/inoculated/training progressive=SED/I/TR_P; training progressive/inoculated/training low intensity TR_P/I/TR_L; training progressive/inoculated/training high intensity TR_P/I/TR_H

Forty-six mice were used to conduct molecular biology experiments, they were divided into five groups: sedentary-sedentary (SED/SED; 8 mice), sedentary-training progressive (SED/TR_P; 8 mice), sedentary-inoculated-sedentary (SED/I/SED; 10 mice), sedentary-inoculated-training progressive (SED/I/TR_P; 10 mice) and training progressive-inoculated-training high intensity (TR_P/I/TR_H; 10 mice). These mice were sacrificed when each mouse lost more than 15% of body weight (cachexia).
All mice were sacrificed by cervical dislocation for blood collection and hind limb posterior muscle groups (the gastrocnemius, plantaris, and soleus muscles), and tumor mass was dissected. Muscles from the right hind limb and half of the tumor mass were frozen in liquid nitrogen and stored at -80°C, whereas the muscles from the left hind limb and the other half of the tumor mass were fixed (acetone, methanol, and water 2:2:1; for 12 h) and embedded in paraffin.

Endurance Training

Trained mice ran 5 days per week on rotarod following specific training protocols. The training protocols have been described in detail in table 1. Sedentary mice did not perform any supervised physical activity.

Table 1. Exercise training protocols.

	TRP		TRL		TRH	
Week	**Time (min)**	**Speed (m/min)**	**Time (min)**	**Speed (m/min)**	**Time (min)**	**Speed (m/min)**
1	15	3.2	30	3.2	60	4
2	30	3.2	30	3.2	60	4
3	30	4	30	3.2	60	4
4	45	4	30	3.2	60	4
5	60	4	30	3.2	60	4
6	60	4.8	30	3.2	60	4

Progressive training (TRP); Low-intensity training (TRL) and High-intensity training (TRH).

Immunofluorescence

Immunofluorescence analysis was performed on tumor, gastrocnemius, plantaris, and soleus muscle slices to detect Hsp60, Pgc1α, and Isolectin expression as a marker of oxidative stress, mitochondrial homeostasis, and vascularization, respectively. The sections were dewaxed in xylene for 30 min at 60 °C and, after immersion in a descending scale of alcohols, rehydrated in distiller water at 23 °C. The deparaffinized sections were incubated in the "antigen unmasking solution" (10 mM tri-sodium citrate, 0.05% Tween-20) for 8 min at 75 °C and treated with a blocking solution (3% BSA in PBS) for 30 min. After, the primary antibodies (anti-Hsp60, rabbit polyclonal ab53109, Abcam; anti-Isolectin mouse monoclonal; anti-Pgc1α, mouse monoclonal) diluted 1:50, were applied, and the sections were incubated in a humidified chamber overnight at 4 °C. Then, the sections were incubated for 1 h at 23 °C with a conjugated secondary antibody (antimouse ATTO-488; anti-rabbit ATTO-647).

Nuclei were stained with Hoescht stain solution (1:1,000, Hoechst 33258, Sigma-Aldrich)and the slides were treated with PBS and coverslipped. The images were captured using a Leica Confocal Microscope TCS SP8 (Leica Microsystems, Wetzlar, Germany). The staining intensity, for Hsp60, Isolectin and PGC1α of each sample, was expressed as the mean pixel intensity (PI) normalized to the cross-sectional area (CSA) using the Leica Application Suite Advanced Fluorescence software.

Immunohistochemistry

Skeletal muscles sections (5 μm) were cut from paraffin-embebbed tessues. The paraffin was removed by the use of xylene for 30 min at 60°C and the sections were rehydrated with alcohols (from 100% to 30%) and left in water for 5 min. The sections were treated with an antigen unmasking solution (10mM tri-sodium citrate, 0.05% Tween-20, pH 6) for 8 minutes at 95°C and transferred in acetone at -20°C for 8 min. The immunostaining was carried out using Histostain®-Plus 3rd Gen IHC Detection Kit after the primary antibodies incubation (anti- Myosin Heavy Chain I, mouse monoclonal A4951-3 DSHB, 3 μg/ml; anti- Myosin Heavy Chain IIb, mouse monoclonal BFF3 DSHB, 3 μg/ml; anti- Myosin Heavy Chain IIa, mouse monoclonal SC71 DSHB, 3 μg/ml; anti- Myosin Heavy Chain IIa/x, mouse monoclonal A474 DSHB, 3 μg/ml), and the nuclei were stained using hematoxylin (Hematoxylin aqueosus formula, N. Cat. S2020, DAKO). The coverslips was placed with an aqueous mounting solution and the images were acquired with an optical microscope (Leica DM 5000 B) connected to a digital camera (Leica DC 300F).

Immunoblotting

Skeletal muscle homogenization was performed with frozen sections either of the posterior muscle group of the hindlimbs (approximately 250 mg each, containing gastrocnemius, soleus, and plantaris muscles) or of the soleus only. Muscles were homogenized by hand (mortar and pestle) in an ice-bath in lysis buffer (200 mM HEPES, 5 M NaCl, 10% Triton X-100, 0.5 M EDTA, 1 M DTT, 0.25 g Na-deoxycholate, 0.05 g SDS) supplemented with Protease Inhibitor Cocktail (Sigma-Aldrich, St. Louis, MO, USA). The homogenates were centrifuged at 13,000xg for 15 minutes at 4 °C and the supernatant fractions (total lysate) were stored at −80 °C. The protein concentrations were quantified spectrophotometrically according to Bradford (Bradford, 1976) using bovine serum albumin (BSA, Sigma-Aldrich) as the standard.

The proteins were separated in 12% SDS-PAGE and electrophoretically transferred to a nitrocellulose membrane 0.45 μm (Bio-Rad Laboratories, Segrate Milano, Italy). The

membrane was incubated in a blocking solution containing 5% BSA in Tris-buffered saline (20 mM Tris, 137 mM NaCl, pH 7.6) containing 0.05% Tween-20 (T-TBS) for 1 h at 23 °C. Next, the membrane was further incubated in a primary antibody, anti-Hsp60 (diluted 1:1,000, mouse monoclonal antibody ab13532, Abcam, Cambridge, UK), or anti-glyceraldehyde-3-phosphate dehydrogenase (GAPDH) diluted 1:3,000, rabbit polyclonal antibody ADI905784, Enzo Life Sciences, Inc. NY, USA). All the primary antibodies were diluted in T-TBS containing 0.5% BSA and incubated overnight at 4 °C. The following day, the membrane was washed with T-TBS and incubated with an HRP-conjugated secondary antibody (anti-rabbit NA934V, or anti-mouse NA931, Amersham Biosciences, NY, USA; for Fig. 6B anti-rabbit A-6154, Sigma ImmunoChemicals, MO, USA) diluted in T-TBS containing 0.5% BSA for 1 h. The detection of the immunopositive bands was performed using ECL Western Blotting Detection Reagent (Amersham Biosciences) according to the manufacturer's instructions. The detected bands were analyzed using ImageJ software version 1.41 (NIH, USA; http://rsb.info.nih.gov/ij). GAPDH bands were checked to control loading.

Statistical analysis

All data are presented as the means ± SD.

The data were analyzed via one-way ANOVA for single measurements or t-test. If a significant difference was detected by the ANOVA, the Bonferroni post-hoc test was carried out. All statistical analyses were performed using GraphPad PrismTM 4.0 software (GraphPad Software Inc., San Diego, CA, USA)and for all of them, the level of statistical significance was set at $p < 0.05$.,

Preliminary Results

Cachexia Model validation

Preliminary evaluations carried out by our research team, focused on the efficacy of the C26 tumor-bearing mice model, documented the effectiveness of cachexia induction in all the groups that were inoculated subcutaneously with a fresh fragment of C26 adenocarcinoma. In particular, it has been found a significant difference in final body weight comparing the tumor-bearing group with the not-tumor bearing mice groups (see table 2).

Groups	SED/SED	SED/TR_P	SED/I/SED	SED/I/TR_P	TR_P/I/TR_H	
Body Weight Initial/Inoculum (g)	26.7±0.9	26.5±1.2	27.8±1.4 *	26.8±1.6 #	26.1±1.4 †	* p=0.0007; # p=0.0002; † p=0.0038
Tumor growth delay (d)	------	------	10.8±1.8	10.4±0.9	10.3±0.4	
Cachexia (d)	------	------	18.6±3.6	16.8±1.8	18.5±3.0	
Final Body Weight (g)	27.6±0.5	26.3±1.1	22.9±1.4 *	21.5±1.0 #	21.8±1.3 †	SED/SED **vs** SED/I/SED, SED/I/TR_P, TR_P/I/TR_H p<0.001 SED/TR_P **vs** SED/I/SED, SED/I/TR_P, TR_P/I/TR_H p<0.001
Hindlimb muscles posterior (g)	0.134±0.04	0.139±0.02	0.122±0.01	0.115±0.01	0.117±0.02	
Tumor (g)	------	------	0.787±0.18	0.536±0.13	0.541±0.10	SED/I/SED **vs** SED/I/TR_P, TR_P/I/TR_H p<0.05

Table 2. The table reports the body weight initial/inoculum (g), tumor growth delay (days), cachexia (days), final body weight (g), hindlimb muscles posterior (g) and tumor (g); (sedentary/sedentary= SED/SED; sedentary/training progressive= SED/TR_P; sedentary/inoculated/sedentary=SED/I/SED; sedentary/inoculated/training progressive=SED/I/TR_P; training progressive/inoculated/training high intensity TR_P/I/TR_H).

In addition, performing several immunohistochemistry staining for the myosin heavy chain on muscles serial section, it has been described the fibers types composition of posterior hindlimb muscles group including gastrocnemius, plantaris and soleus muscles, along with a statistical analysis of the atrophy degrees for every fiber-types in these muscles (see figure 1).

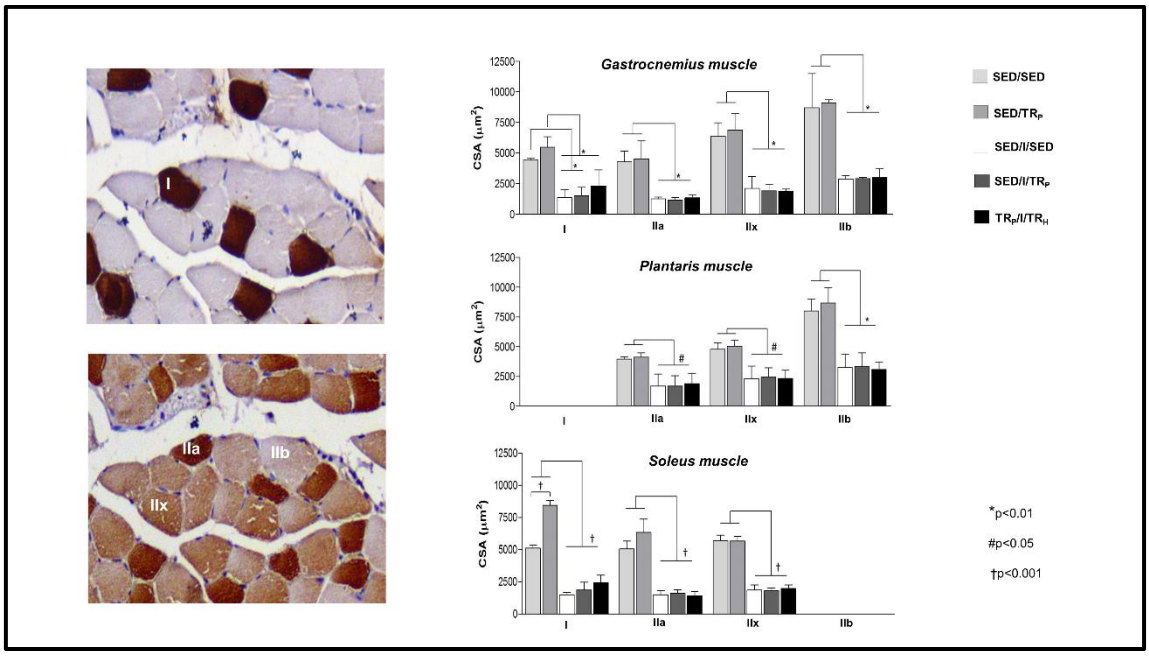

Figure1: the figure shows the immunohistochemistry staining for the myosin heavy chains (I, IIa, IIx, and IIb) in gastrocnemius, plantaris, and soleus muscles. The muscles cross section area analysis documents the cachectic effect of the C26 colon adenocarcinoma on skeletal muscles. (sedentary/sedentary= SED/SED; sedentary/training progressive= SED/TR_P; sedentary/inoculated/sedentary=SED/I/SED; sedentary/inoculated/training progressive=SED/I/TR_P;training progressive/inoculated/training high intensity TR_P/I/TR_H).

The physical exercise prolongs the average survival and slow down cachexia onset in C26 tumor-bearing mice

The effectiveness of exercise training in prolonging the average survival of tumor bearing mice was confirmed by the comparison between the average survival of trained tumor-bearing mice with the sedentary groups. Interestingly, both TR_P/I/TR_L (training progressive-inoculated-training low intensity) and TR_P/I/TR_H (training progressive-inoculated-training high intensity) groups showed a gain in survival compared with the sedentary mice that underwent to tumor inoculation and subsequent training or sedentary condition (SED/I/TR_P and SED/I/SED respectively). Although a significant impact on the average survival has been documented in relation to the high-intensity training protocol (TRP/I/TRH) effect. Moreover, the high intensity protocol

counteracted the cachectic effect of the C26 colon adenocarcinoma delaying the cachexia onset (see figure 2).

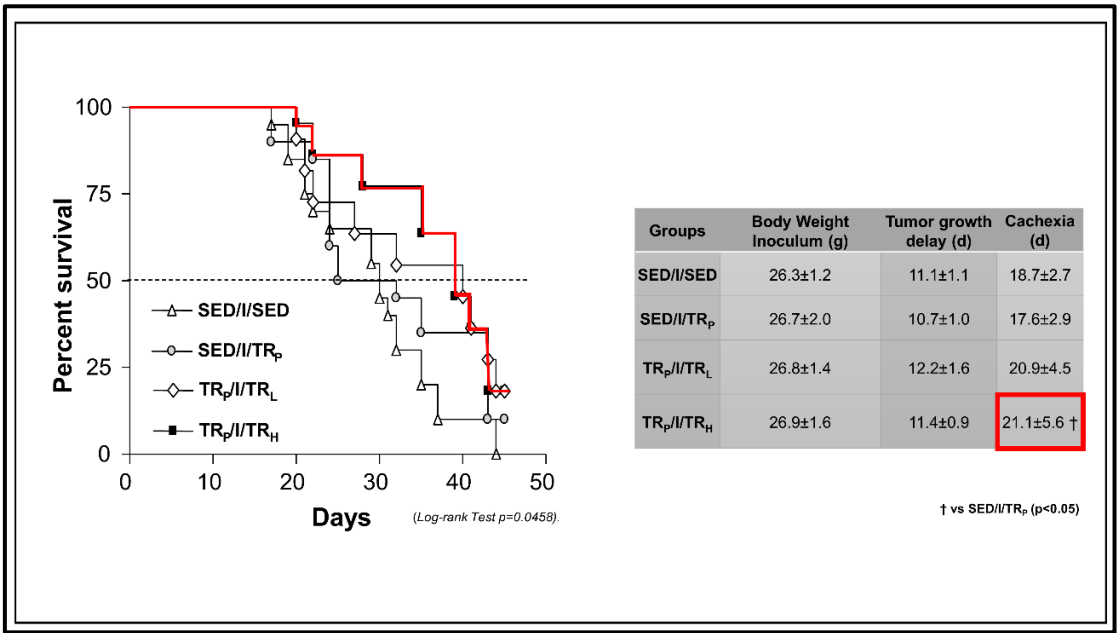

Groups	Body Weight Inoculum (g)	Tumor growth delay (d)	Cachexia (d)
SED/I/SED	26.3±1.2	11.1±1.1	18.7±2.7
SED/I/TR_P	26.7±2.0	10.7±1.0	17.6±2.9
TR_P/I/TR_L	26.8±1.4	12.2±1.6	20.9±4.5
TR_P/I/TR_H	26.9±1.6	11.4±0.9	21.1±5.6 †

† vs SED/I/TR_P ($p<0.05$)

Figure 2: the figure shows the graph of the survival curve and a table reporting the body weight (g) at the tumor inoculation, the tumor growth delay (days) and the cachexia onset (days) of the mice groups (sedentary/inoculated/sedentary=SED/I/SED; sedentary/inoculated/training progressive=SED/I/TR_P; training progressive/inoculated/training low intensity TR_P/I/TR_L; training progressive/inoculated/training high intensity TR_P/I/TR_H).

Results

Exercise training reduces the tumor growth triggering the tumor cells apoptosis and inhibiting their proliferation

The analysis of the data collected from immunohistochemistry assay, targeting the expression of the Proliferating Cell Nuclear Antigen (PCNA) in tumor sections, documented that the high intensity training inhibits the tumor cells proliferation in tumor-bearing mice. Comparing the percentage of PCNA positive cells between the SED/I/SED, SED/I/TR_P, and TR_P/I/TR_H groups it has been found an higher percentage of proliferating cells in the tumor of SED/I/SED and SED/I/TR_P groups than the tumor of TR_P/I/TR_H group. Further, the TUNEL assay demonstrated a significant increase in apoptotic processes in tumor mass collected from TR_P/I/TR_H mice group compared to the SED/I/SED group. Both of these processes led to a significant decrease of the tumor weight in SED/I/TR_P, and TR_P/I/TR_H group compared to the SED/I/SED group (see figure 3).

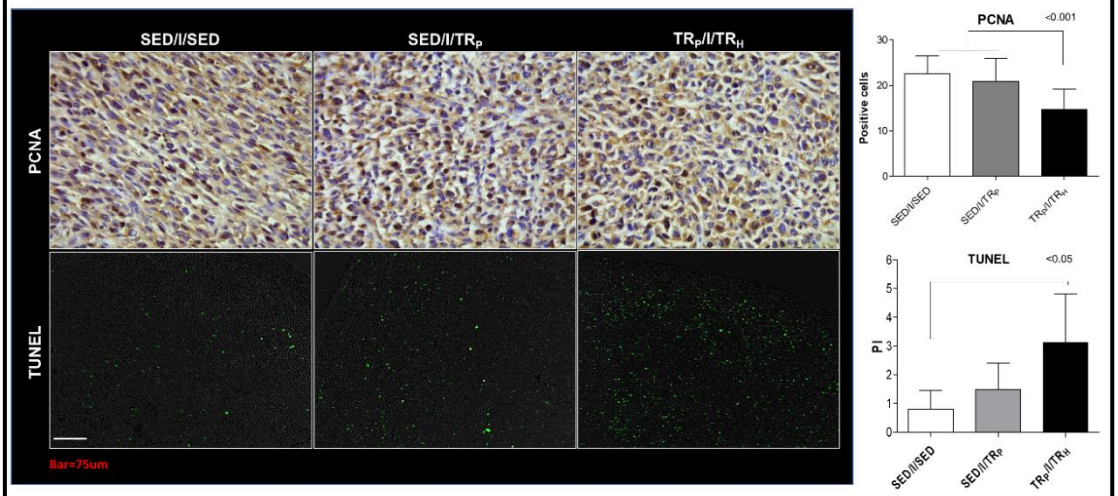

	SED/I/SED	SED/I/TR_P	TR_P/I/TR_H	
TUMOR (g)	0.787±0.18	0.536±0.13	0.541±0.10	SED/I/SED vs SED/I/TR_P, TR_P/I/TR_H p<0.05

Figure 3: the figure shows the results of the immunohistochemistry assay for the PCNA detection and the TUNEL assay in tumor sections form SED/I/SED, SED/I/TR_P, and TR_P/I/TR_H groups. The table reports the tumor weight with the statistical comparison between the mice groups (sedentary/inoculated/sedentary= SED/I/SED; sedentary/inoculated/training progressive=SED/I/TR_P; training progressive/inoculated/training high intensity TR_P/I/TR_H).

Tumor: Hsp60 and Isolectin immunofluorescences

The immunofluorescence analysis carried out on the tumor slices highlighted a significant decrease in Hsp60 signal in the sedentary tumor-bearing mice compared to the trained tumor-bearing mice. Conversely, the sedentary/inoculated/sedentary group showed a strong immunoreactivity for Isolectin, which was significatively higher than the trained tumor-bearing groups (see figure 4).

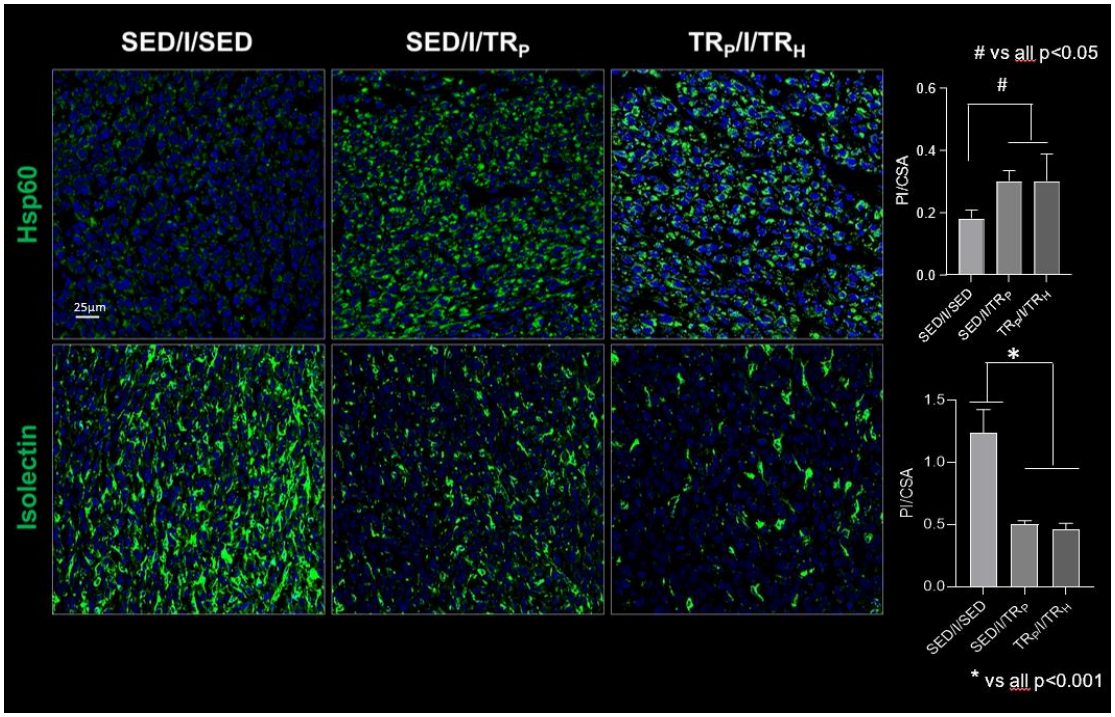

Figure 4. The figure shows Hsp60 and Isolectin immunofluorescence images and the graphs reporting the results of the statistical analysis carried out on tumor sections (Sedentary/Inoculated/Sedentary = SED/I/SED; Sedentary/Inoculated/Training progressive= SED/I/TR_P; Training progressive/Inoculated/Training high intensity = TR_P/I/TR_H).

Skeletal muscles: Hsp60 and Isolectin immunofluorescences

Hsp60 immunofluorescence

The immunofluorescences analysis showed a significant increase in immunoreactivity of Hsp60 in soleus muscle from the mice that underwent the progressive training before the tumor inoculation and then trained with the high-intensity protocol ($TR_P/I/TR_H$), compared with the sedentary mice (SED/SED). The same significant increase was observed in red gastrocnemius muscles from $TR_P/I/TR_H$, compared with the SED/SED group. No relevant differences between the different groups in plantaris and white gastrocnemius were observed (see figure 5).

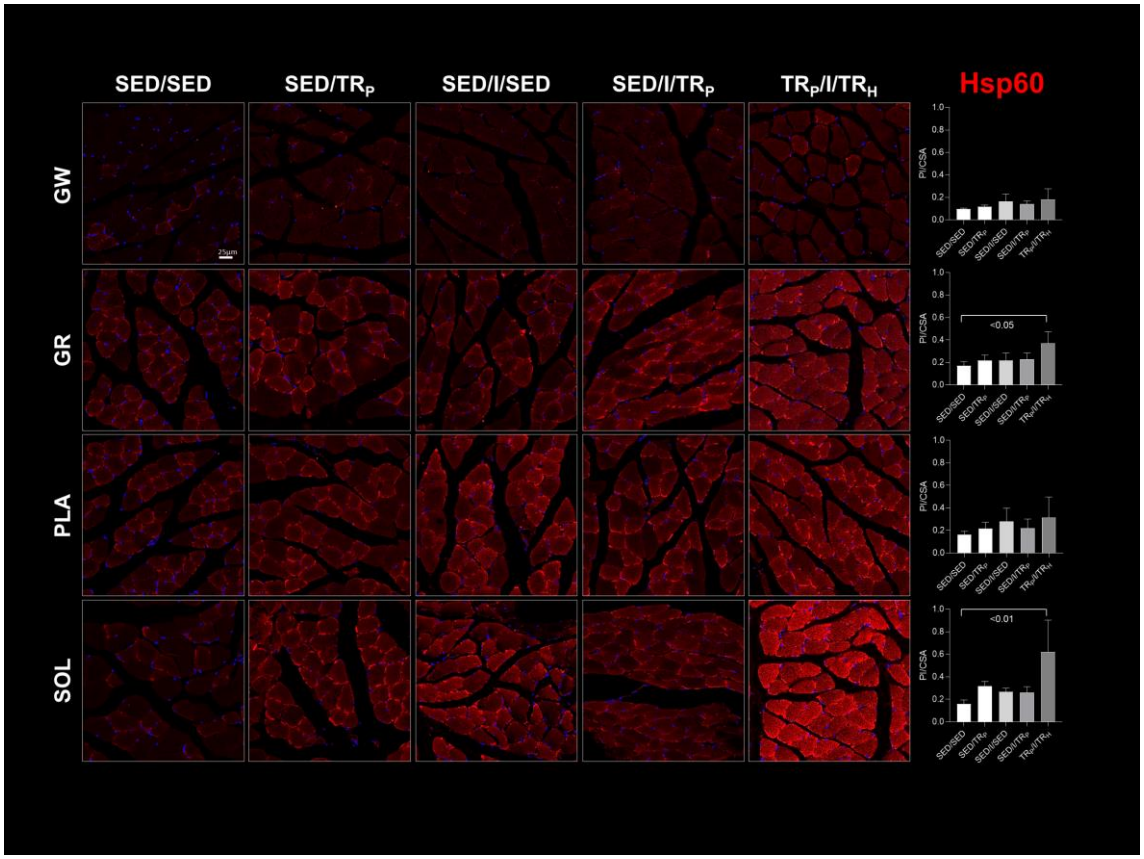

Figure 5. The figure shows the Hsp60 immunofluorescence images together with the graphs reporting the Hsp60 signal quantification and the statistical analysis (Soleus = SOL; Plantaris = PLA; Gastrocnemius white part = GW; Gastrocnemius red part = GR; Sedentary/Sedentary= SED/SED; Sedentary/Training progressive= SED/TR_P Sedentary/Inoculated/Sedentary = SED/I/SED; Sedentary/Inoculated/Training progressive= $SED/I/TR_P$; Training progressive/Inoculated/Training high intensity = $TR_P/I/TR_H$)

Isolectin immunofluorescence

The immunoreactivity of Isolectin was significantly increased in white gastrocnemius and soleus muscles from SED/I/TR_P and TR_P/I/TR_H groups compared to the not-bearing tumor groups. In plantaris and red gastrocnemius muscles from TR_P/I/TR_H group has beendocumented an higher level of Isolectin compared to the SED/SED group, while the amount of this protein was significantly increased in the same muscles of the SED/I/TR_P group compared to both SED/SED and SED/TR_P groups (see figure 6).

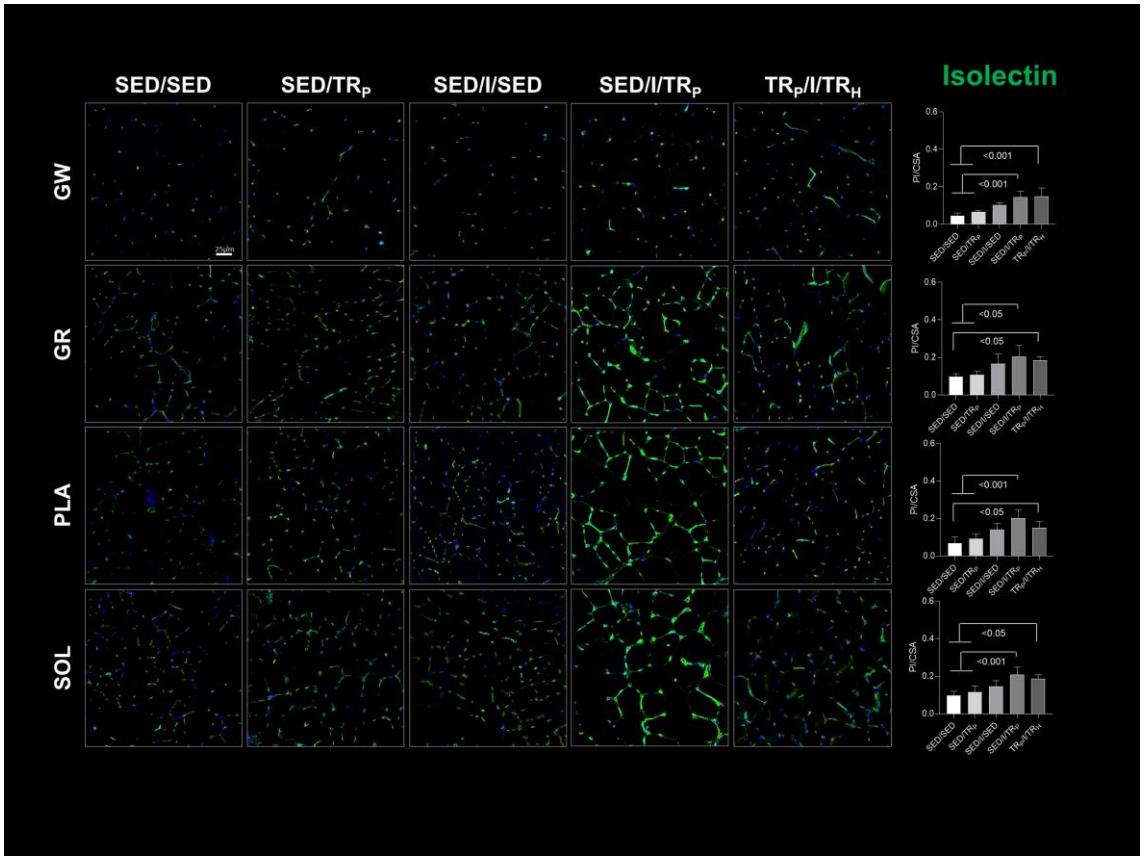

Figure 6. Isolectin immunoreactivity: The figure shows the Isolectin immunofluorescence images along with the graphs reporting the Isolectin signal quantification and the statistical analysis (Soleus = SOL; Plantaris = PLA; Gastrocnemius white part = GW; Gastrocnemius red part = GR; Sedentary/Sedentary= SED/SED; Sedentary/Training progressive= SED/TR_P Sedentary/Inoculated/Sedentary = SED/I/SED; Sedentary/Inoculated/Training progressive = SED/I/TR_P; Training progressive/Inoculated/Training high intensity = TR_P/I/TR_H).

PGC1α immunofluorescence

Skeletal muscle slices were used to perform immunofluorescence analysis for PGC1α. Among the different mice groups studied, the greater and more significant increase of PGC1 signal was reported in soleus, plantaris, and red gastrocnemius muscles of the tumor-bearing trained groups (SED/I/TR_P and TR_P/I/TR_H) when compared with the sedentary mice (SED/SED). No significant differences were found in the white gastrocnemius of all mice groups (see figure 7).

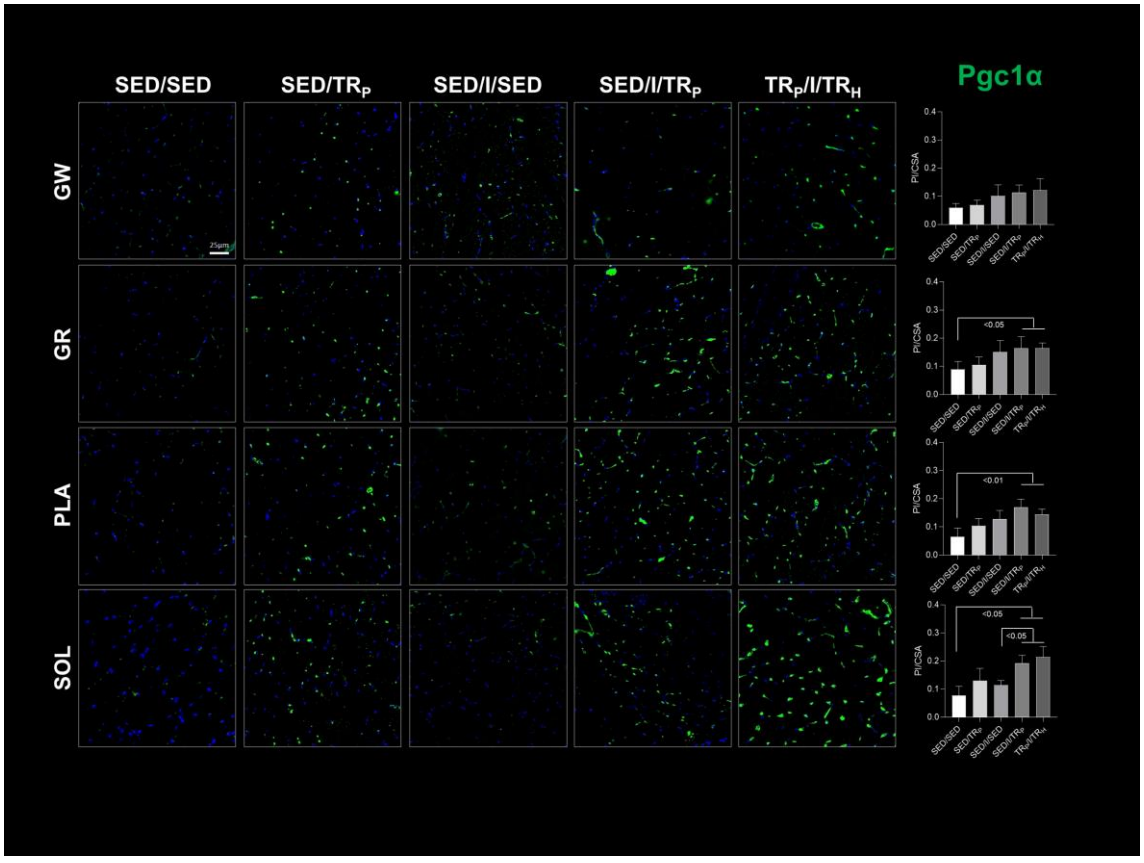

Figure 7. Pgc1α immunofluorescence: The figure shows the Pgc1α immunofluorescence images along with the graphs reporting the Pgc1α signal quantification and the statistical analysis (Soleus = SOL; Plantaris = PLA; Gastrocnemius white = GW; Gastrocnemius red = GR; Sedentary/Sedentary= SED/SED; Sedentary/Training progressive= SED/TR_P Sedentary/Inoculated/Sedentary = SED/I/SED; Sedentary/Inoculated/Training progressive SED/I/TR_P; Training progressive/Inoculated/Training high intensity = TR_P/I/TR_H).

Double immunofluorescences: preliminary results

Preliminary double immunofluorescences on skeletal muscles slideshave been performed to evaluate the matching ratio between Hsp60 with Isolectin andHsp60 with PGC1α. The results have been shown in figures 8 and 9, although more studies are needed to clarify the colocalization ratio.

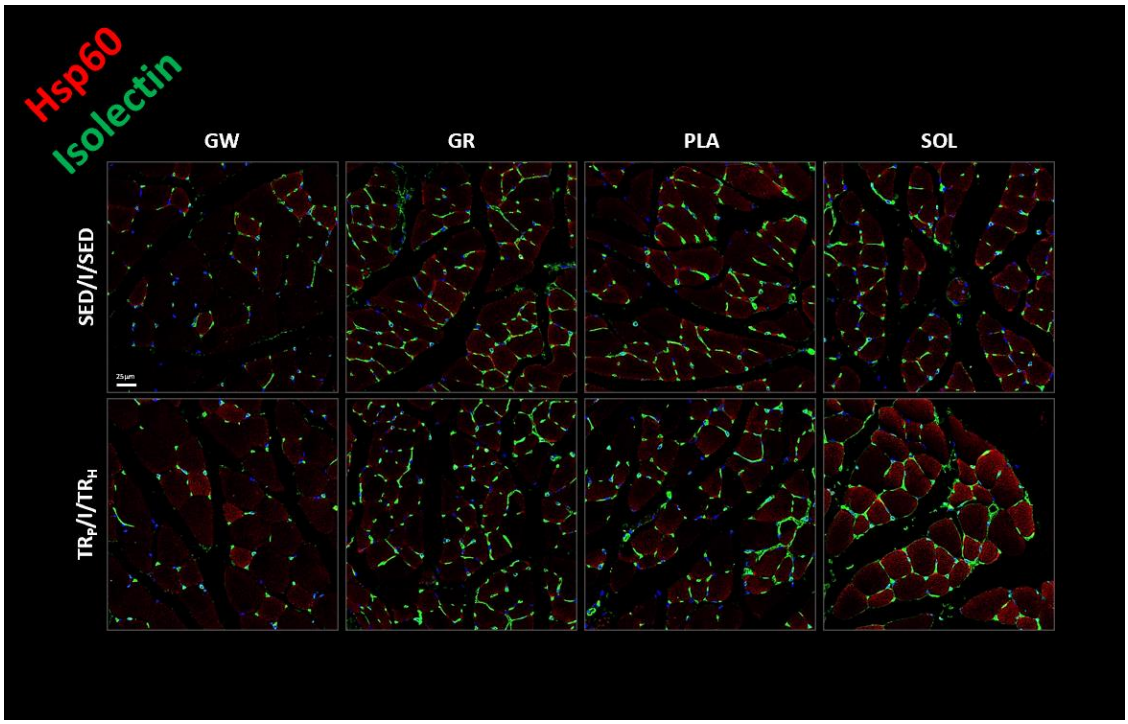

Figure 8. Hsp60 and Isolectin doble immunofluorescence: Soleus = SOL; Plantaris = PLA; Gastrocnemius white = GW; Gastrocnemius red = GR; Sedentary/Inoculated/Sedentary = SED/I/SED; Training progressive/Inoculated/Training high intensity = $TR_P/I/TR_H$.

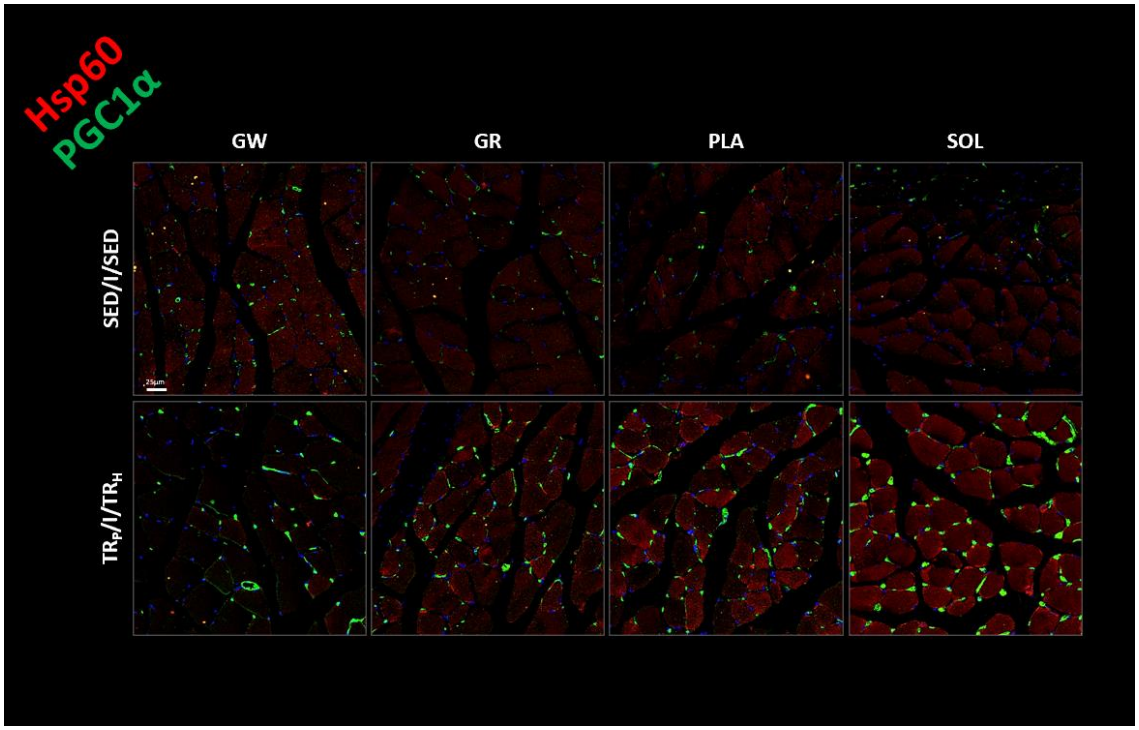

Figure 9. Hsp60 and Pgc1α colocalization: Soleus = SOL; Plantaris = PLA; Gastrocnemius white = GW; Gastrocnemius red = GR; Sedentary/Inoculated/Sedentary = SED/I/SED; Training progressive/Inoculated/Training high intensity = $TR_P/I/TR_H$.

Discussion

The effectiveness of physical exercise on healthy life is well established by several studies although its potential role in improving different pathological conditions is still under investigation as well as the underlying mechanism through which it exerts its beneficial effect. Exercise training, by modulating various organ functions, promotes cross-talk between tissues maintaining overall body homeostasis. Pathological conditions are characterized by the primary involvement of an organ that over time interferes with the functioning of other remote organs through the modulation of signaling factors. Since inflammation is the most common shared step in several diseases, it has been suggested that inflammatory (pro or anti-inflammatory) cytokines

represent the systemic mediators interconnecting different organs and thus regulate the whole body homeostasis (Mangano G.D. et al., 2022).

In oncology, it has long been recognized, since Virchow's initial observation in 1863, that chronic inflammation plays a relevant role in the development and progression of tumors (Balkwill, F., & Mantovani, A. 2001). This data has been extensively documented in the scientific literature, with many studies confirming the link between chronic inflammation and cancer (Coussens LM & Werb Z. 2002). It is widely accepted that chronic inflammation can promote tumor initiation, progression, and metastasis through various mechanisms, including the release of inflammatory mediators and growth factors, as well as the activation of oncogenic signaling pathways (Balkwill F. 2006; Gupta SC. et al., 2012). On the other hand, exercise training represents the most efficient not-pharmacological intervention able to decrease the inflammatory state by the modulation of the inflammatory cytokines (Metsios, G. S. et al., 2020), and its overall effectiveness result in improved patients outcome including lifespan prolongment (Irwin, M. L. et al., 2008; Dieli-Conwright, C. M. et al., 2018).

The present project draws inspiration from unpublished data collected by our research team, which documented a significant improvement in quality of life among tumor-bearing mice that underwent aerobic exercise training, consistent with findings in the scientific literature. In particular, the comparison between three training protocols, differing for intensity (low, progressive and high intensity training) and administration timing (pre tumor inoculation or pre and post tumor inoculation), revealed a strong effectiveness of the training protocols characterized by the administration pre and post tumor inoculum ($TR_P/I/TR_L$ and $TR_P/I/TR_H$) in increasing the average survival. Considering the lack of significant differences between the $TR_P/I/TR_L$ and $TR_P/I/TR_H$ protocols in survival results, the subsequent experiments were carried out excluding the $TR_P/I/TR_L$ mice group.

Tumor and clinical data analysis documented that exercise training induced a significant increase in cells apoptosis along with cellular proliferation inhibition resulting in a significant reduction of the tumor weight, and cachexia onset. Moreover, accordingly to the previously mentioned background, exercise training significantly reduced the tumor inflammatory cytokine level including IL1, IL6, and TNFα as confirmed by the qRT-

PCR assay. All these data together offer a great contribution to the research field studying the potential role of exercise training in cancer patients. However, often the critical condition of cancer patients makes it difficult to use as a therapeutic intervention.Thus, the study of the molecular response to the training can provide insight to develop specific molecules mimicking the exercise effect.

Recently, a growing interest has been focused on a protein family known as Heat Shock Proteins (HSPs), these proteins play an important role in protecting and restoring the correct conformation of other proteins inside cells (Cappello F. et al., 2013). Dysfunction of chaperonin proteins can lead to the accumulation of misfolded proteins, which can have toxic effects on cells and cause diseases (Cappello F. et al., 2013). A recent study documented altered expression of HSP60 in colorectal cancer tissues and its association with poor prognosis and aggressive tumor behavior. The authors also discussed the possible mechanisms underlying the oncogenic functions of HSP60, including its ability to regulate tumor cell proliferation, migration, invasion, and resistance to apoptosis (Javid H. et al., 2022). Moreover, Cömert C. and colleagues reported that the reduction of HSP60 expression leads to an increase in reactive oxygen species production and alteration of mitochondrial function. The authors used a Hsp60 deficient-model to test the efficacy of a compound known to improve mitochondrial functionality, rapamycin and observed that treatment with this molecule partially restores mitochondrial functionality altered by HSP60 deficiencies.

Interestingly, a study by Barone R. et al., (2013) investigated the expression of heat shock protein 60 (Hsp60) in skeletal muscle tissue following endurance training. The authors observed a significant increase in the expression of Hsp60 in skeletal muscle tissue after 6 weeks of endurance training. Furthermore, the study also demonstrated that the increase in Hsp60 expression was associated with an increase in peroxisome proliferator-activated receptor gamma coactivator 1α1 (PGC-1α1) expression, a transcriptional coactivator known to regulate mitochondrial biogenesis and oxidative metabolism. These findings suggested that Hsp60 may play a role in the adaptive response of skeletal muscle tissue to endurance training and that Hsp60 induction may be a potential target for enhancing the benefits of endurance training also in cancer disease (Barone R. et al., 2013). In line with these findings, a qualitative and quantitative evaluation of immunofluorescence demonstrated that endurance training

significantly induced the expression of Hsp60 protein in a mouse model of colon adenocarcinoma. The increased amount of protein was accompanied by a significant increase in its mRNA levels, as confirmed by other data obtained from western blotting and qRT-PCR assays performed by our research team. Furthermore, we observed that our training protocols interfere with the tumor vascularization processes, reducing the capillarity density, as demonstrated by a lower level of isolectin immunoreactivity in tumor sections from sedentary tumor-bearing mice compared to trained groups (SED/I/TR_P and TR_P/I/TR_H).

The same increasing in Hsp60 protein level has been documented in skeletal muscles of the cachectic mice of the trained groups. In particular, the high intensity training protocol induced a strong increase of Hsp60 in red gastrocnemius and soleus muscles although no significant differences have been observed in white gastrocnemius and plantaris muscles. Therefore, these results are consistent with Barone and colleagues that reported a fiber-type specificity for Hsp60, with a greater response observed in type I oxidative muscle fibers in relation to endurance training. Moreover, also the immunofluorescence analysis of Pgc1α confirmed that the induction of Hsp60 expression in type I muscle fibers after endurance training was associated with an increase in the expression of peroxisome proliferator-activated receptor gamma coactivator 1 alpha (PGC-1α), a key regulator of mitochondrial biogenesis and oxidative metabolism in skeletal muscle.

Differently from what was observed in trained mice tumors, the rate of muscular vascularization was significantly increased in trained tumor-bearing mouse groups compared to sedentary and sedentary/trained control groups.

Therefore, the collective data suggest that endurance training may have a potential role in promoting adaptations in the context of cancer disease. These adaptations include the reduction of oxidative stress through the modulation of Hsp60 and PGC-1α, the inhibition of tumor growth through the activation of apoptosis and the deceleration of cellular proliferation, as well as the arrest of tumor vascularization.

However, more studies are needed to identify the most effective exercise interventions for different types of cancer, as well as the optimal duration, frequency, and intensity of exercise required to achieve therapeutic benefits. Overall, a better understanding of the

mechanisms by which physical exercise exerts its positive effects on both health and disease will have important implications for effective exercise-based interventions as well as for the development of new pharmacological approaches.

Conclusion

The positive effects of physical exercise on overall health have been widely established by numerous studies. However, its potential role in improving different pathological conditions is still being explored, and the underlying mechanisms through which it exerts its beneficial effects are not yet completely understood. Although there is evidence supporting the positive impact of physical exercise on several disease outcomes, including cancer, cardiovascular disease, and metabolic disorders, further research is required to elucidate the precise mechanisms responsible for these benefits. In addition, more studies are needed to identify the most effective exercise interventions for different pathologies, as well as the optimal duration, frequency, and intensity of exercise required to achieve therapeutic benefits. Overall, a better understanding of the mechanisms by which physical exercise exerts its positive effects on health will have important implications for the development of effective exercise-based interventions for various diseases.

Study 2: Refining Cisplatin Chemotherapy

Abstract

Chemotherapy together with radiotherapy and surgery is one of the main therapeutic approaches to oncologic diseases. Among the several cytotoxic agents, cisplatin represents a milestone in the chemotherapy treatment of several tumors such as ovarian, neck, and colon cancer although its relevant side-effects are progressively limiting its use. In recent years several studies have investigated the appropriate dosage of cisplatin in animal models suggesting that high doses of cisplatin are needed to achieve a significant inhibitory effect on the growth of the tumor, while lower doses may have limited efficacy (Damrauer et al. 2018; Sakai et al. 2014; Arita M et al., 2021).

In line with these evidences, the objective of the current study was to evaluate the effectiveness of cisplatin treatment at a dosage of 2.5 mg/Kg in reducing tumor weight and inducing side effects, particularly cachexia in the animal model. Additionally, in order to optimize cisplatin therapy by identifying the lowest effective dose while minimizing side effects, we carried out multiple experiments in both 2D and 3D models. Finally, we compared these models to detect differences in cellular responses to cisplatin treatment.

In vivo experiments were carried out on thirty female Balb-c mice seven-week-old, while in vitro experiments were performed in triplicate and repeated five times using 3-D spheroids and 2-D monolayer C26 cell culture. The mice were subcutaneously inoculated with 2x106 colon adenocarcinoma cells (C26) and after ten days of tumor growth, it was administered i.p. 2,5 mg/Kg of cisplatin for four days. The C26 cells in both in vitro experiments (2-D and 3-D models) were treated with a solution of cisplatin 1μM for 24 hours. In all the experiments was evaluated the percentage of early apoptotic cells using Annexin-V labelling while the percentage of late-apoptotic cells and the cells cycle were studied by the use of Propidium iodide. Further, the tumors and the skeletal muscles (anterior tibialis, gastrocnemius, and extensor digitorum longus) weights were considered as outputs measure of the cisplatin anti-cancer effect and side-

effect induction, respectively. The cisplatin anti-cancer efficacy in vitro experiments was evaluated by counting the C26 cells number after 24 hours of treatment.

The results documented a significant reduction in tumor growth after cisplatin treatment in both the models (in vivo and in vitro 2-D model) although it has been reported an increased weight loss percentage in treated mice. Further, the percentage of early-apoptotic C26 cells in relation to cisplatin administration was significantly increased whereas no differences have been found in late-apoptotic C26 cells. Moreover, the statistical analysis revealed that data from repeated experiments are subjected to stochastic variability. Finally, the preliminary results of the cell cycle evaluation suggest a different cellular behaviour in relation to the cisplatin treatment.

These findings suggest that improving the administration of cisplatin chemotherapy could expand the range of treatment options available to oncologists. These findings give valuable guidance for selecting appropriate chemotherapy models.

Introduction

Chemotherapy is one of the main therapeutic approach to the oncologic diseases together with radiotherapy and surgery. The first use of the term “chemotherapy” came from the beginning of the 20thcentury referring to chemical compounds with a selective efficacy on different organisms rescuing the host’s tissues. Recently, this term has been used in the oncology field as synonymous with cytotoxic drugs losing thus the concept of selective toxicity, although several efforts have been done to improve the specificity of the cancer tissue targeting (Ellis H.; 2015).

The aim of chemotherapy is to interfere with cell proliferation and induce apoptosis in tumor mass, preventing the invasion and metastasis processes. Currently, it has been developed several cytotoxic drugs that differ in their mechanism of action (Tilsed CM et al., 2022). In particular, the alkylating agents, including the platinum analogues, act by

intercalating alkyl groups between the two strands of DNA preventing its replication and, inducing an alteration in RNA transcription (Karati D et al 2022).

The purine and pyrimidine antimetabolites are converted to analogues of cellular nucleotides and included in the nucleic acid (DNA, RNA) inhibiting different enzymes involved in DNA synthesis (Parker W. B. 2009). Other compounds exert a selective inhibition of certain enzymes such as the topoisomerase inhibitors that block the DNA unwinding enzymes (Delgado JL et al 2018). The last class of cytotoxic agents includes the molecules that arrest cell division by interfering with the microtubular architecture in the mitotic spindle (Stanton RA et al., 2011).

All mechanisms targeted by the cytotoxic agents are critical in both healthy and cancerous conditions. Thus, a variety of side effects are reported in scientific literature. Since highly proliferating cells are primarily affected by anti-cancer drug therapy, the most common side-effects of chemotherapy include myelosuppression, mucositis, alopecia, fatigue, and infertility. In addition to these non specific side-effects, the chemotherapeutic agents show an organ specific toxicity in relation to their metabolism and excretion (Amjad MT. et al ., 2023).

In line with the goal of the chemotherapy treatment, three ways of treatment administration have been reported: neoadjuvant, adjuvant, and combined (Tanvetyanon T. et al., 2005). Neoadjuvant therapy consists of a preliminary chemotherapeutic approach before the surgical treatment, aimed to reduce the tumor size allowing the exeresis. When the chemotherapy treatment is administered after the surgical approach, it is labeled as adjuvant and it is aimed to damage the residual cancer cells and to keep suppressing the tumor growth. However, in a variety of cases, a combined approach, such as adding radiotherapy, has been found effective to arrest tumor progression (Zhang L. et al., 2013).

All cytotoxic agents can be administered as a single drug or in a multidrug combination. The combined multidrug therapy offers several advantages such as the reduction of the dose needed to obtain the anti-tumor effect of each drug and thus also their toxicity. Furthermore, the multidrug approach including different not-overlapping mechanisms of action, prevents the development of resistant clones (Amjad MT. et al ., 2023).

Cisplatin

Cisplatin is a chemotherapeutic drug used in the treatment of various types of cancer, including testicular, ovarian, bladder, and lung cancer (Dasari, S., & Tchounwou, P. B. 2014).

The chemical structure of cisplatin consists of a square planar arrangement of atoms, with two chloride ions and two amine groups coordinated to a central platinum atom (Rosenberg B et al., 1969).

Once cisplatin enters the cell, it undergoes hydrolysis, forming positively charged species that can react with DNA to form intrastrand and interstrand cross-links, which block DNA replication and transcription, eventually leading to apoptosis (Behmand, B. et al., 2020). Cisplatin can also affect cell signaling pathways, such as the MAPK and NF-kB pathways, leading to cell cycle arrest and apoptosis. In addition, it can cause oxidative stress and mitochondrial dysfunction, further contributing to cell death (Wang, X. L. et al., 2021).

Cisplatin is known to activate multiple cell signaling pathways that contribute to its cytotoxic effects. The JNK pathway is one of the pathways activated by cisplatin, which leads to cell cycle arrest and apoptosis (Galluzzi et al., 2012). The MAPK pathway is another important pathway that is affected by cisplatin. This pathway can lead to cell death via both caspase-dependent and caspase-independent mechanisms (Galluzzi et al., 2012). The NF-kB pathway is also involved in cisplatin-induced cell death. Activation of this pathway can lead to the transcription of pro-apoptotic genes, resulting in cell death (Galluzzi et al., 2012). Additionally, the p53 pathway is activated by cisplatin-induced DNA damage, leading to apoptosis and cell cycle arrest (Galluzzi et al., 2012).

The identification of these signaling pathways has shed light on the complex mechanisms underlying cisplatin-induced cytotoxicity. The activation of these pathways by cisplatin represents a potential target for the development of combined therapies that can enhance the efficacy of cisplatin-based chemotherapy.

Several studies investigated the role of oxidative stress and mitochondrial dysfunction in cisplatin-induced cell death. Cisplatin can increase the production of reactive oxygen

species (ROS), leading to oxidative stress and mitochondrial dysfunction (Yu, W. et al., 2018). This, in turn, can lead to the activation of apoptotic pathways and cell death. Furthermore, cisplatin-induced ROS can also activate autophagy, which can either promote cell survival or contribute to cell death, depending on the context (Magnano, S. et al., 2021).

Platinum-based chemotherapy, such as cisplatin, has been extensively used for the treatment of various cancers. However, the effectiveness of cisplatin is often limited by the development of drug resistance. The development of drug resistance is a complex process that involves various molecular mechanisms, including alterations in DNA repair pathways, changes in drug transport and metabolism, alterations in signaling pathways, and changes in apoptosis and cell cycle regulation. Several studies have been conducted to investigate the molecular mechanisms underlying cisplatin resistance, and these studies have led to the identification of several key molecular targets that may be involved in the development of resistance.

One important target that has been identified is the DNA repair pathway. Cisplatin exerts its cytotoxic effects by forming DNA adducts, which can cause DNA damage and lead to cell death. However, cancer cells can develop resistance to cisplatin by enhancing their DNA repair capacity, which can prevent the accumulation of DNA damage and cell death. Several studies have shown that cisplatin-resistant cells have increased expression of DNA repair proteins, such as ERCC1, XPA, and BRCA1, which may contribute to their resistance (Rocha CR et al., 2018; Siddik Z. H. 2003; Köberle B. et al., 2021).

Another important mechanism of cisplatin resistance is alterations in drug transport and metabolism. Cisplatin enters cells through copper transporters and organic cation transporters (OCTs) and is then transported out of cells by ATP-dependent transporters, such as P-glycoprotein (P-gp) (Amable L. 2016). Alterations in the expression or activity of these transporters can affect the intracellular accumulation of cisplatin and contribute to drug resistance. Several studies showed that the overexpression of P-gp is associated with cisplatin resistance in various cancer types (He C. et al., 2019; Shen et al., 2012).

Changes in signaling pathways have also been implicated in the development of cisplatin resistance. For example, the PI3K/Akt/mTOR pathway has been shown to be involved in cisplatin resistance by promoting cell survival and preventing apoptosis (Peng DJ et al., 2010). In addition, alterations in the expression of several other signaling molecules, such as JNK, MAPK, and NF-κB, have also been confirmed to contribute to cisplatin resistance (Achkar IW et al., 2018).

Finally, alterations in apoptosis and cell cycle regulation have also been implicated in the development of cisplatin resistance. Cisplatin induces apoptosis by activating the intrinsic pathway of apoptosis, which is mediated by the Bcl-2 family of proteins. Alterations in the expression of Bcl-2 family members or other apoptotic regulators, such as p53 and survivin, have been shown to contribute to cisplatin resistance (Galluzzi et al., 2012; Siddik, 2003).

Thus the development of cisplatin resistance is a complex process that involves multiple molecular mechanisms. Understanding these mechanisms is critical for the development of effective strategies to overcome drug resistance and improve the efficacy of cisplatin-based chemotherapy.

Besides the cisplatin resistance issue also several side effects of the cisplatin treatment limit the use of this cytotoxic agent.

Nephrotoxicity is one of the most common and severe side effects of cisplatin treatment, which can lead to renal dysfunction and even acute kidney injury (Pabla and Dong, 2008). Several mechanisms have been proposed for cisplatin-induced nephrotoxicity, including oxidative stress, inflammation, and apoptosis (McSweeney KR et al., 2021). Ototoxicity is another common side effect of cisplatin treatment, which can lead to hearing loss and tinnitus. The mechanism of cisplatin-induced ototoxicity is not completely understood, but it is thought to involve oxidative stress, inflammation, and apoptosis in the cochlea (Sheth S, et al., 2017). In addition to these side effects, cisplatin can also cause gastrointestinal toxicity, peripheral neuropathy, and myelosuppression (Avan A. et al., 2015; Kanat O. et al., 2017; Basu A. et al., 2015). To mitigate these side effects, several strategies have been developed, such as the use of hydration and diuretics to prevent nephrotoxicity and the use of otoprotective agents to prevent ototoxicity (Hayati F. et al., 2015; Yu D. et al., 2020). The development of novel

cisplatin analogs and combined therapies may also reduce the incidence and severity of these side effects while maintaining the efficacy of cisplatin-based chemotherapy.

Cisplatin-induced cachexia

Cisplatin-induced cachexia is a multifactorial condition that is caused by various mechanisms, including inflammation, muscle damage, and altered muscle metabolism. Inflammation is a key feature of cisplatin-induced cachexia and is thought to contribute to the loss of muscle mass and function (Tisdale MJ., 2002). Several studies have shown that cisplatin treatment leads to increased production of inflammatory cytokines, such as interleukin-6 (IL-6), tumor necrosis factor-alpha (TNF-α), and interleukin-1 beta (IL-1β) in skeletal muscle and circulation (Kim GT. et al., 2022; Brierley DI et al., 2019). Cisplatin-induced TNF-α and IL-1 overexpression activate the IKK complex and phosphorylate inhibitors of NF-κB, causing their degradation and nuclear translocation of activated NF-κB. This induces the expression of MAFbx/atrogin-1 and MuRF1, leading to muscle wasting and cachexia (Webster JM. Et al., 2020; Damrauer JS. Et al., 2018). Additionally, IL-6 induced by cisplatin can bind to its receptor IL-6R, causing homodimerization of gp130 and activating JAKs, which results in the suppression of protein synthesis through activation of transcription factors of the STAT family (Moreira-Pais A et al., 2018).

Further, cachexia cisplatin-related seems to involve impaired mitochondrial biogenesis and mass which are crucial mechanisms for muscle mass homeostasis (Sirago, G. et al., 2017). In particular, the authors documented low levels of PGC-1α probably due to the impairment of the PI3K-Akt-mTOR signaling pathway in rats treated with cisplatin. Interestingly, a study by Huot et al. examined the effects of PGC1α overexpression on cisplatin-induced cachexia in the skeletal muscles of mice. It was demonstrated that PGC1α overexpression preserves muscle mass and function, reduces body weight loss and muscle atrophy, inhibits inflammation, and increases mitochondrial energy production (Huot JR. et al., 2022). This suggests that PGC1α may represent a potential therapeutic target for preventing or treating cachexia in cancer patients undergoing cisplatin chemotherapy.

Another pathological mechanism suggested underlying the cachectic effect induced by cisplatin, also involves dysregulation in calcium control. It has been reported that high levels of calcium can induce ubiquitin-proteasome-dependent proteolysis through the activation of calpains (Sorimachi H. & Ono Y. 2012). Additionally, high levels of calcium within the cell interfere with proper mitochondrial function through the protein Bax, whose activation induces cell apoptosis (Agrawal A. et al., 2018). Thus, calcium dysfunction could be closely related to cisplatin-induced muscle impairment. The disruption of calcium homeostasis could impair the functionality of calcium-dependent proteases and phospholipases that are essential for various muscle functions (Conte E. et al., 2020). These effects induced by cisplatin could contribute to calcium overload in the cytoplasm of muscle cells, detrimentally interfering with muscle maintenance and function.

In conclusion, cisplatin-induced cachexia is a complex and multifactorial condition that involves inflammation, muscle damage, and altered muscle metabolism. The development of effective therapies for cisplatin-induced cachexia is crucial to improve the quality of life and clinical outcomes of cancer patients undergoing chemotherapy.

Research Aims

In recent years several studies have investigated the appropriate dosage of cisplatin in animal models. Overall, many studies suggest that the appropriate dosage of cisplatin in animal models may vary depending on the specific study design and animal species used (Perše M. 2021). However, the majority of the studies suggest that higher doses of cisplatin (ranging from 3 mg/kg to 5 mg/kg) have a significant inhibitory effect on the growth of the tumor, while lower doses may have limited efficacy (Damrauer et al. 2018; Sakai et al. 2014; Arita M et al., 2021)

In line with this context, the objective of the current investigation was to assess the effectiveness of cisplatin treatment at a dosage of 2.5 mg/Kg in reducing tumor weight and inducing side effects, particularly cachexia. Additionally, in order to optimize cisplatin therapy by identifying the minimum effective dose while minimizing side effects, we carried out multiple experiments in both 2D and 3D models. Finally, we compared these models to detect differences in cellular responses to cisplatin treatment.

Materials and Methods

Animal

The experiments were carried out using thirty 7-week-old female mice (BALB/c AnNHsd). All mice were maintained at a constant temperature of 21 ± 2 °C with controlled lighting (12-hrs light-dark cycle) and were allowed free access to food and water. All the mice were subcutaneously inoculated with 2 x 10^6 C26 cells in 100 µl of Phosphate Buffered Saline (PBS) per mouse.

After 10 days from the C26 cells inoculation, the mice were divided into two groups: C26 (not-treated) and C26+CIS (treated with cisplatin). This latter group was treated for 4 days with cisplatin at the concentration of 2,5 mg/Kg, while the C26 group received 100 µl of saline solution.

All animal experiments were approved by the Committee on the Ethics of Animal Experiments of the University of Sorbonne and adhered to the recommendations in the Guide for the Care and Use of Laboratory Animals by the USA National Institute of Health (NIH). All experiments were performed in the Sorbonne Universitè, Laboratory B2A Biological Adaptation and Ageing (CNRS UMR 8256 - INSERM ERL U1164 - Sorbonne).

Cell culture

C2C12: mouse myoblasts (from ATCC CRL-1772™) were maintained in DMEM high glucose, GlutaMAX™ Supplement (Gibco, Thermo fischer) containing, 4.5 g/l glucose supplemented with 10% heat-inactivated Fetal Bovine Serum (FBS), 1000 UI/ml penicillin, 1000 UI/ml streptomycin, and 2 mM L-Glutamine at 37 °C in humidified air containing 5% CO2.

C26: Colon carcinoma cell line (ATCC CRL-2638) was maintained in Corning™ RPMI 1640 medium with L-Glutamine (Corning™ 10-040-CV) supplemented with 10% heat-inactivated Fetal Bovine Serum (FBS), 1000 UI/ml penicillin, 1000 UI/ml streptomycin at 37 °C in humidified air containing 5% CO2.

Cisplatin *in vitro* experiments: microscopic analysis after DAPI staining

C26 cells were cultured in 12-well plates ($3x10^5$ cells for each well) for 24h in 1ml of RPMI + FBS 10% + P/S (Penicillin/ Streptomycin) 1%. Subsequently, the culture medium was removed and replaced with 1ml of RPMI + FBS 10% + P/S 1% + Cisplatin 1µM (Sigma Aldrich, Merk, PHR1624-200MG, CAS-No: 15663-27-1). After 24 hours the culture medium was removed and 3 washes were performed for 5 minutes with PBS. The cells were incubated with 500µl PBS + DAPI (dil. 1:5000) for 5 minutes at RT in dark. Finally, 3 washes were done for 5 minutes with PBS, and the plate was left to air dry ready to be observed under the microscope for counting the nuclei.

Cisplatin *in vitro* experiments 2D-model: cytofluorimetric analysis for Annexin-V and Propidium Iodide

C26 cells were cultured in the 12-well plates ($3x10^5$ cells for each well) for 24h in 1ml of RPMI + FBS 10% + P/S 1%. Then the culture medium was removed and replaced

with 1ml of RPMI + FBS 10% + P/S 1% + Cisplatin 1µM for 24h. After the cisplatin treatment, the cells were detached, washed and resuspended in 100 µl of Annexin Buffer 1X, 5µl FITC ANNEXIN-V (component A) and 1µl of the PI working solution 100 µg/mL (FITC Annexin V/Dead Cell Apoptosis Kit for Flow Cytometry; FITC annexin V Component A; Propidium iodide Component B; 5X annexin-binding buffer Component C; Invitrogen, Catalog n°: V13242, Stored at 4° C). The samples were incubated at room temperature for 15 minutes in the dark and then were added 400 µl of Annexin-binding buffer 1X. The samples were analyzed by flow cytometry (figure 10).

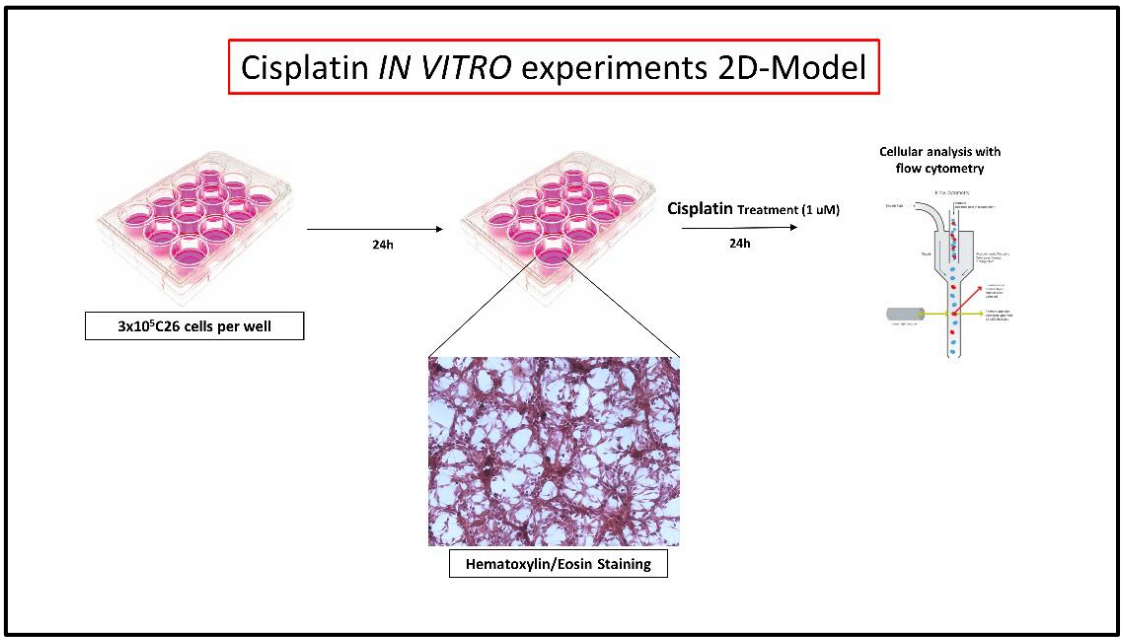

Figure 10. The figure shows a schematic view of the cisplatin in vitro 2-D model experiments.

Cisplatin *in vitro* experiments 3D-model: cytofluorimetric analysis for Annexin-V and Propidium Iodide

C26 cells (1x106) were cultured in a 15ml falcon tube for 72 hours with 3ml of RPMI + FBS 10% + P/S 1%. Cisplatin treatment was carried out for 24 hours in 3ml of RPMI + FBS 10% + P/S 1%+ cisplatin 1µM. The cells were detached and washed with PBS. Subsequently, the cells were resuspended in 100 µl of Annexin Buffer 1X, 5µl FITC

ANNEXIN-V (component A), and 1µl of the PI working solution 100 µg/mL (FITC Annexin V/Dead Cell Apoptosis Kit for Flow Cytometry; FITC annexin V Component A; Propidium iodide Component B; 5X annexin-binding buffer Component C; Invitrogen, Catalog n°: V13242, Stored at 4° C). The samples were incubated at room temperature for 15 minutes in the dark and after adding 400 µL of Annexin-binding buffer 1X the samples were analyzed by flow cytometry (figure 11).

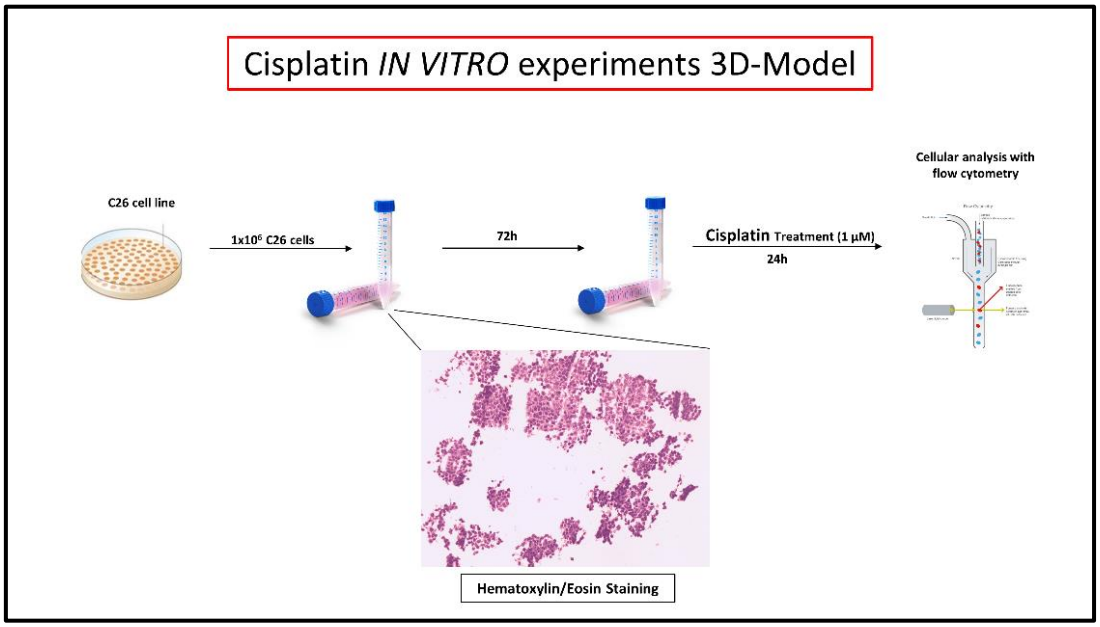

Figure 11. The figure shows a schematic view of the cisplatin in vitro 3-D model experiments.

Cisplatin *in vivo* experiments 3D-model: cytofluorimetric analysis for Annexin-V and Propidium Iodide

The C26 colon cancer cells were cultured with RPMI + FBS 10% + P/S 1% in T75 flasks, when the cells reached 80-90% of confluence, were detached with trypsin 1x and counted to reach the concentration of $2x10^6$ cells in 100µl PBS to be inoculated subcutaneously in each BALB/c mouse (cAnNCrl, 7-week-old females, Charles river). A total of 30 mice were used. The animals were divided into two groups, 15 for the

control group i.e. mice that received the inoculum of C26 tumor cells but were not treated (C26), and 15 mice inoculated with C26 tumor cells and treated with cisplatin (C26+CIS). The animals were kept under constant control to observe the development of the tumor mass, after 10 days from the inoculation the treatment was carried out by intraperitoneal injections of Cisplatin 2.5 mg/Kg for 4 days. On day 15 the mice were weighed and sacrificed to isolate, gastrocnemius (GA) muscle, and tumor mass. The muscles were weighed, one part frozen in liquid nitrogen and one part included in OCT (Tissue-Tek® OCT cryoembedding compound, compound 4583, Labtech) for subsequent studies. The tumor mass instead after being removed and weighed was cut with scissors in petri dish 100mm with PBS and placed in digestion medium (4 mL of tumor digestion medium: 500 µl Collagenase/Hyaluronidase + 3,5 mL RPMI 1640 medium) and subsequently incubated at 37°C for 30 minutes on a rotating platform. Using a 70 µm nylon strainer in a 50 mL conical tube the sample was filtered and resuspended in 30ml of PBS + FBS 2%, centrifuged at 300 x g for 10 minutes at RT. Once the supernatant was removed, the sample was resuspended in 5ml of PBS. Using the kit; FITC Annexin V/Dead Cell Apoptosis Kit for Flow Cytometry, isolated cells were counted (5 x 105 tumor cells) and resuspended in 100 µl Annexin Buffer 1X + 5µl FITC ANNEXIN-V (component A) + 1µl of the 100 µg/mL PI working solution, cells were incubated at RT for 15 minutes in the dark and finally resuspended in 400 µl of annexin-binding buffer 1X and analyzed by flow cytometry (figure 12).

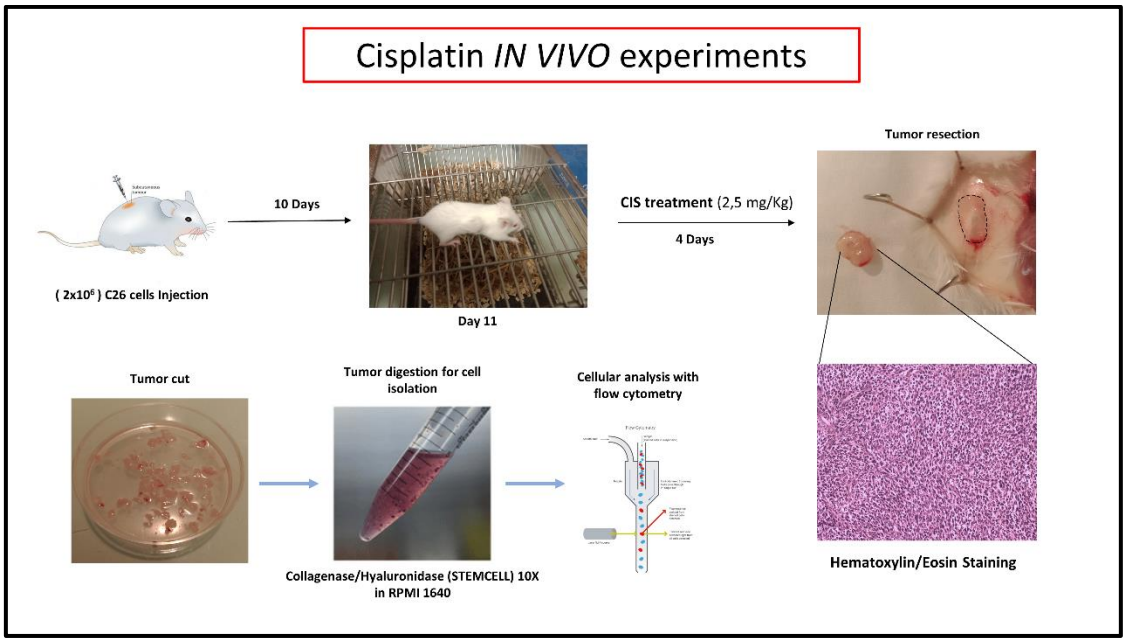

Figure 12. The figure shows a schematic view of the cisplatin in vivo experiments.

Cisplatin *in vitro* experiments 2D-model: Flow cytometric analysis of cell cycle with propidium iodide DNA staining

The C26 cell line was maintained in RPMI 1640 medium with L-Glutamine (Corning™ 10-040-CV) supplemented with 10% heat-inactivated Fetal Bovine Serum (FBS), 1000 UI/ml penicillin, 1000 UI/ml streptomycin at 37 °C in humidified air containing 5% CO2. C26 cells were plated at the density of 3X105 cells in a 12-wells plate and after the adhesion (24 hours), they were treated with a solution of cisplatin 1µM (RPMI+10% FBS+1%S/P+Cisplatin) for 24 hours. The cells were washed in PBS, detached with trypsin 1x for 5 min, and after the addition of RPMI+FBS10%, they were centrifuged at 400 g for 5 min at 4°C. The supernatant was discharged and the pellet was washed in PBS and centrifuged at 400 g for 5 min at 4°C. The cells were fixed in cold 70% ethanol added dropwise to the pellet while vortexing, to minimize clumping for 20 minutes at -20°C. The ethanol was spun out by centrifuging the pellet at 850 g for 5 min at 4°C and after two washes in PBS, the cells were treated with 50 µl of ribonuclease stock solution 100 µg/ml.

Finally, the samples were incubated with 200 µl of PI (from 50 µg/ml stock solution) for 15 min at RT in the dark and analyzed by flow cytometry (PI maximum emission of 605 nm).

The forward scatter (FS) and side scatter (SS) were measured to identify single cells and, pulse processing was used to exclude cell doublets from the analysis. This was also achieved either by using pulse area vs. pulse width or pulse area vs. pulse height.

Cisplatin *in vitro* experiments 3D-model: Flow cytometric analysis of cell cycle with propidium iodide DNA staining

The C26 cell line was maintained in RPMI 1640 medium with L-Glutamine (Corning™ 10-040-CV) supplemented with 10% heat-inactivated Fetal Bovine Serum (FBS), 1000 UI/ml penicillin, 1000 UI/ml streptomycin at 37 °C in humidified air containing 5% CO2. C26 cells were plated at the density of $1X10^6$ cells in a 15ml falcon tube and after 72 hours, they were treated with a solution of cisplatin 1µM (RPMI+10% FBS+1%S/P+Cisplatin) for 24 hours. The cells were washed in PBS, detached with trypsin 1x for 5 min, and after the addition of RPMI+FBS10%, they were centrifuged at 400 g for 5 min at 4°C. The supernatant was discharged and the pellet was washed in PBS and centrifuged at 400 g for 5 min at 4°C. The cells were fixed in cold 70% ethanol added dropwise to the pellet while vortexing, to minimize clumping for 20 minutes at -20°C. The ethanol was spun out by centrifuging the pellet at 850 g for 5 min at 4°C and after two washes in PBS, the cells were treated with 50 µl of ribonuclease stock solution 100 µg/ml.

Finally, the samples were incubated with 200 µl of PI (from 50 µg/ml stock solution) for 15 min at RT in the dark and analyzed by flow cytometry (PI maximum emission of 605 nm).

The forward scatter (FS) and side scatter (SS) were measured to identify single cells and, pulse processing was used to exclude cell doublets from the analysis. This was also achieved either by using pulse area vs. pulse width or pulse area vs. pulse height.

Results

Cisplatin *in vivo* experiments : Cisplatin treatment reduces tumor growth in cachexia animal model

The data analysis of the tumor weights collected *in vivo* experiments, revealed a significant impact of cisplatin treatment in reducing the tumor weight (see figure 13).

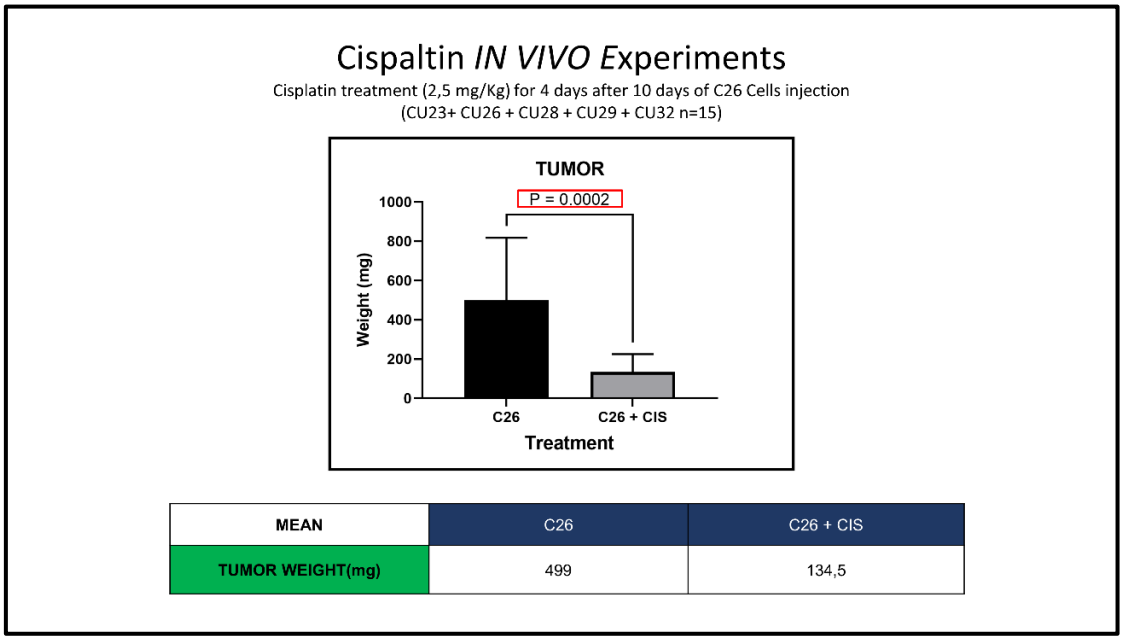

MEAN	C26	C26 + CIS
TUMOR WEIGHT(mg)	499	134,5

Figure 13. The figure shows the graph reporting the comparation between the tumor weight in treated and untreated groups (C26+CIS and C26 respectively). The significance of the t-student analysis was established at the p-value< 0.05 (P<0,05). The table shows the mean values of the tumor weight (mg) of the mice groups.

Data provided by the body weight analysis documented a significant increase in weight loss percentage in the group of tumor-bearing mice treated with cisplatin compared to the not-treated tumor-bearing mice group (see figure 14).

Further, the carcass weight, considered as the final body weight less the tumor weight, was significantly higher in tumor-bearing mice not-treated with cisplatin than in the treated tumor-bearing mice group. (see figure 14).

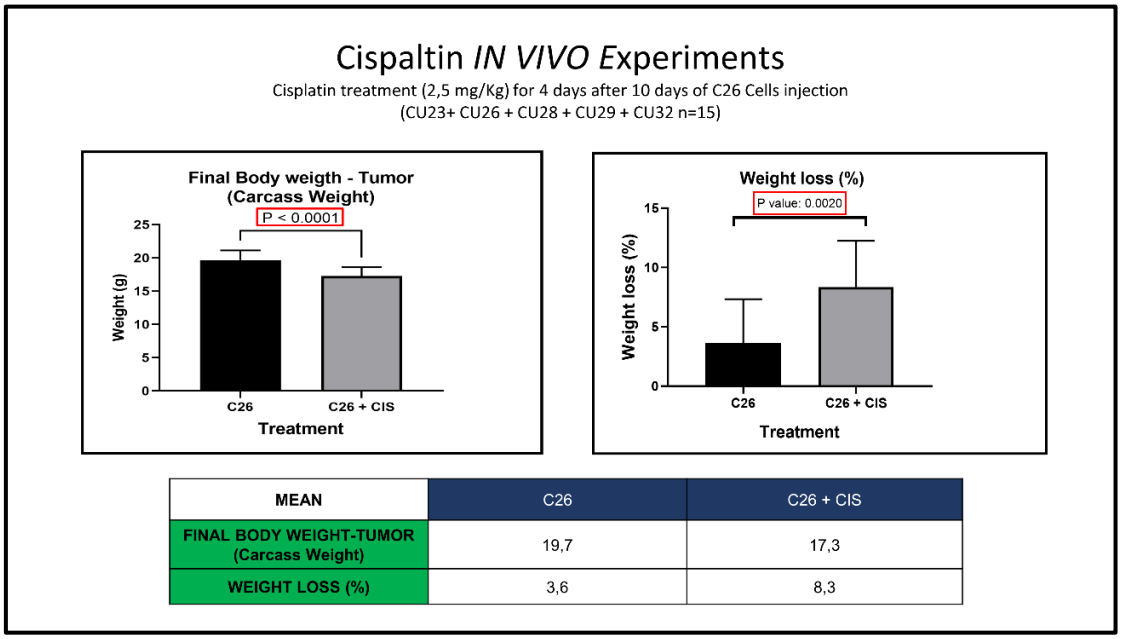

MEAN	C26	C26 + CIS
FINAL BODY WEIGHT-TUMOR (Carcass Weight)	19,7	17,3
WEIGHT LOSS (%)	3,6	8,3

Figure 14. The figure shows the graphs reporting the comparison between the carcass weight (Final body weight less the tumor weight), and the weight loss percentage in treated and untreated groups (C26+CIS and C26 respectively). The significance of the t-student analysis was established at the p-value< 0.05 (P<0,05). The table shows the mean values of the final body weight less tumor weight (Carcass weight) and the weight loss percentage (%) in the mice groups.

Interestingly, we also documented a significant decrease in spleen weight of the treated mice group while no differences were reported in skeletal muscles weight (Tibialis anterior; gastrocnemius; extensor digitorum longus) comparing both mice groups (see figure 15).

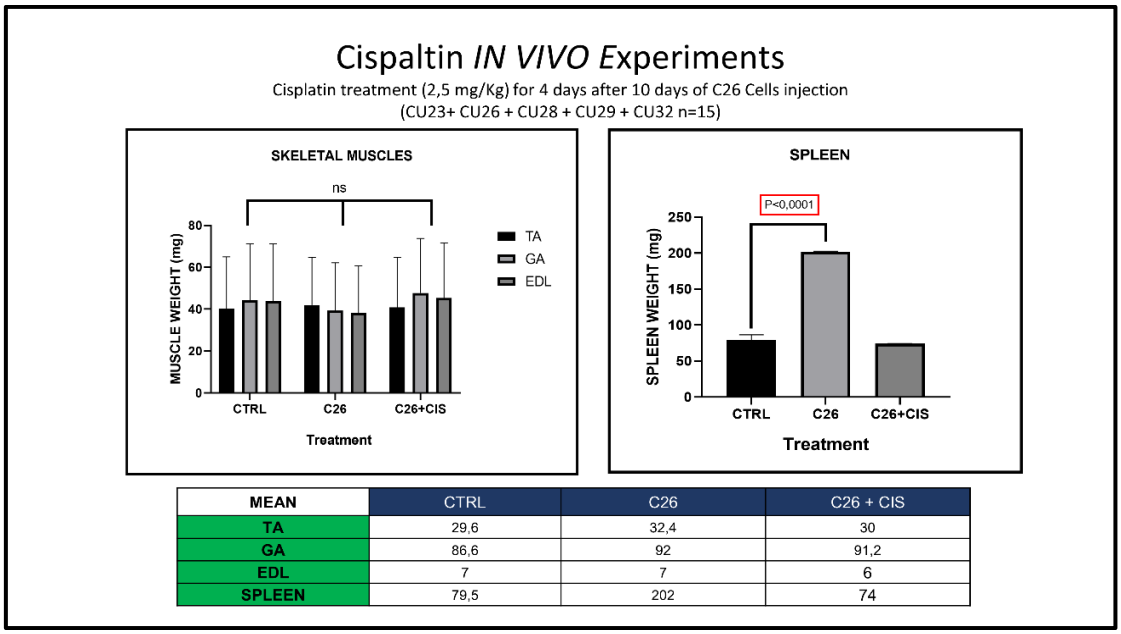

MEAN	CTRL	C26	C26 + CIS
TA	29,6	32,4	30
GA	86,6	92	91,2
EDL	7	7	6
SPLEEN	79,5	202	74

Figure 15. The figure shows the graphs reporting the skeletal muscles weights (TA= Tibialis Anterior; GA= Gastrocnemius; EDL= Extensor Digitorum Longus), and the spleen weight comparison between the control (CTRL= without tumor), treated and untreated groups (C26+CIS= treated mice; C26= untreated mice). The table shows the weight mean values of the skeletal muscles (TA, GA and EDL), and the spleen of the three groups (CRTL, C26 AND C26+CIS). The significance of the t-student analysis was established at the p-value< 0.05 (P<0.05).

Cisplatin *in vitro* experiments: DAPI staining and cell number counting in 2D-model

The anti-tumor effect of the cisplatin treatment *invitro* experiment was studied by counting the number of DAPI-stained cells per microscopic field. Preliminary results from our research team documented a significant reduction in the number of DAPI-stained cells from the C26 cell culture after cisplatin treatment, compared to the not-treated C26 cell culture (see figure 16).

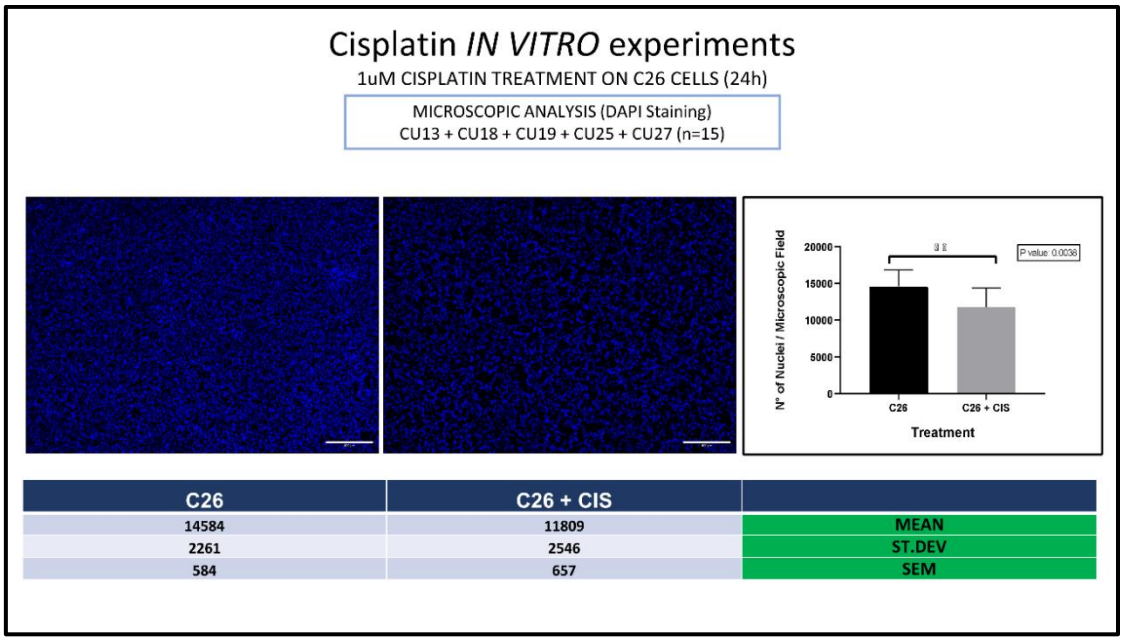

Figure 16. The figure shows the microscope images of C26 cells treated and untreated (C26+CIS and C26 respectively) with cisplatin 1µM and subsequently stained with DAPI, magnification 10x; the graph shows the comparison between treated and untreated groups in number of DAPI stained cells per microscopic field . The significance of the t-student analysis was established at the p-value< 0.05 (P<0,05). The table reports the mean values, standard deviation and SEM of the number of DAPI stained cells per microscopic field in treated and untreated C26 cells.

Replicate experiments are subject to stochastic variability

The statistical analysis of 5 *in vivo* experiments (n=15) revealed an high variability between the different experiments. In particular, we reported a standard deviation variability between the analysis of the samples from the not-treated mice (C26). Further, the p value of every single experiment differed from the others experiments although, the p value trend tended to the significant level increasing the samples size (n=15) (see figure 17 A). The same results were achieved by a preliminary in vitro experiments that our research team carried out (see figure 17 B).

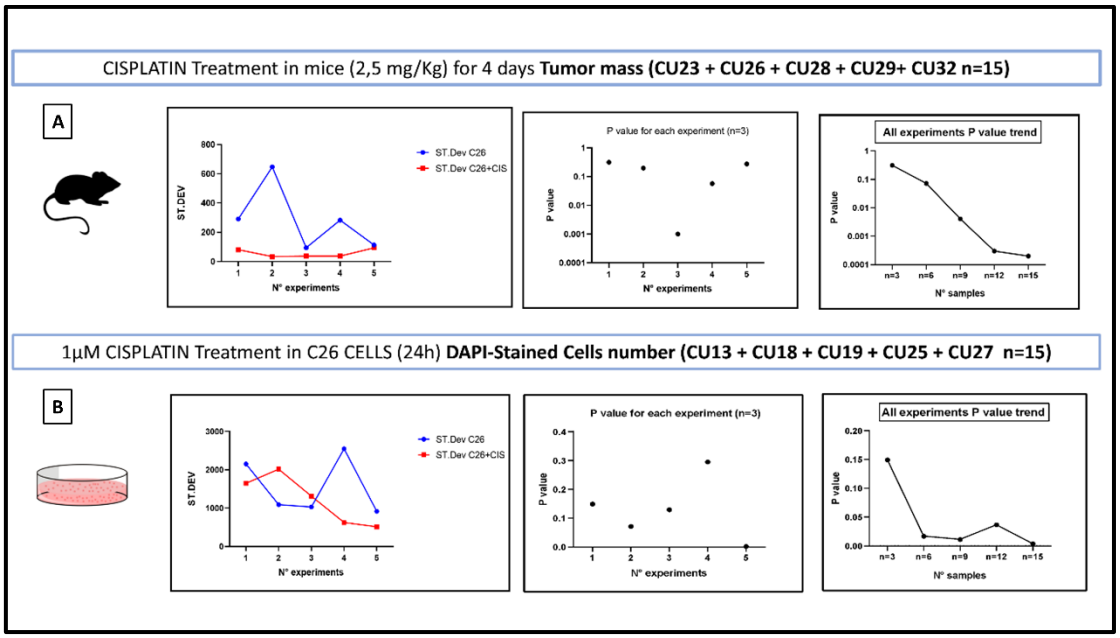

Figure 17. A) The figure shows the graphs reporting the standard deviation (ST.DEV), p values and p value trend of five *in vivo* experiments evaluating the tumor mass (C26=C26 untreated mice; C26+CIS=mice treated with cisplatin). **B)** The figure shows the graphs reporting the standard deviation (ST.DEV), p values and p value trend of five *in vitro* experiments evaluating the number of DAPI stained cells (C26=C26 untreated cells; C26+CIS=C26 cells treated with cisplatin).

Targeting early and late apoptosis in cisplatin chemotherapy models

The anti-tumor effect of the cisplatin treatment here reported has been further studied by analyzing the processes of apoptosis. In both models, in vivo and in vitro it has been studied the early and late apoptosis by the use of Annexin V and Propidium Iodide (PI) labeling, respectively.

The Annexin V assay, a classic technique for detecting apoptosis, is the most suitable methodcommonly used to detect apoptosis by flow cytometry. Annexin V is oneprotein that has a high affinity for phosphatidylserine (PS) a phospholipidplasma membrane. One of the first features of apoptosis is translocationof PS from the inner to the outer leaflet of the plasma membrane, exposingso PS to the external environment. Annexin V binds to PS exposed on the surfaceand identifies cells in an early stage of apoptosis before other assaysbased on DNA fragmentation.

Conversely, Propidium iodide (PI) cannot penetrate thecell membranes, therefore it enters exclusivelyin permeabilized or dead cells labeling thus the necrotic and late apoptotic cells.

In Vivo model: Targeting early and late apoptosis in cisplatin chemotherapy

Cytofluorometric analysis documented that the percentage of C26 cells annexin-V positive was significantly increased after cisplatin treatment (see figure 18). Conversely, the PI labeling did not present any differences between treated and not-treated tumor-bearing mice (see figure 19).

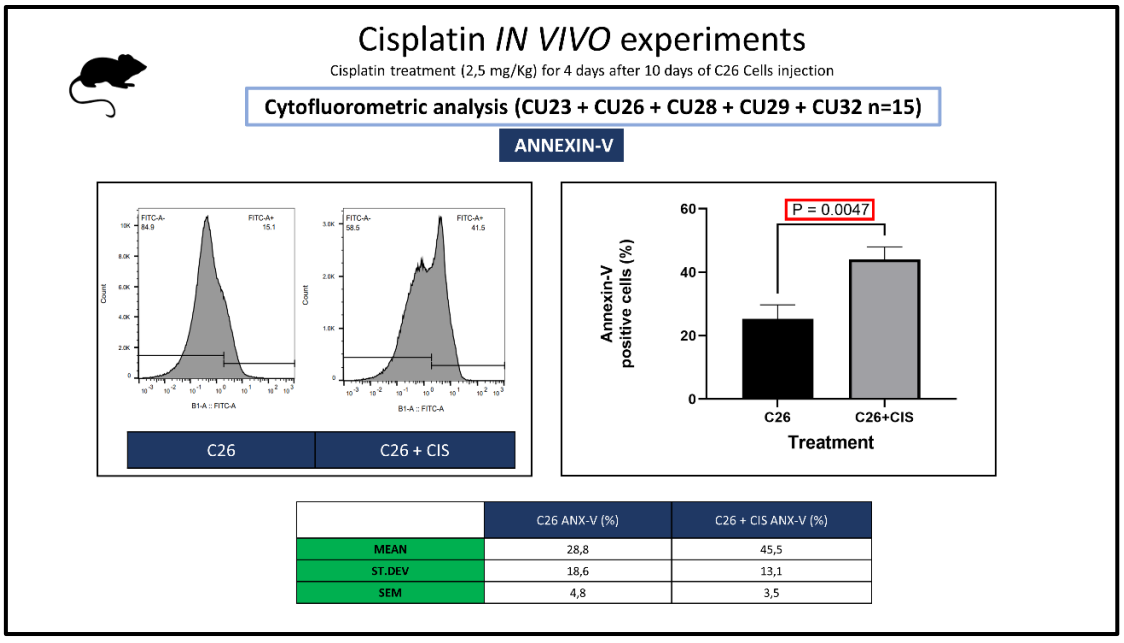

	C26 ANX-V (%)	C26 + CIS ANX-V (%)
MEAN	28,8	45,5
ST.DEV	18,6	13,1
SEM	4,8	3,5

Figure 18. The figure shows the flow cytometry analysis of Annexin-V assay; the graph shows the comparison between the treated and untreated mice groups (C26+CIS and C26, respectively) in percentage of annexin-V positive cells. The table reports the mean values, standard deviation and SEM of the percentage of annexin-V positive cells in treated and untreated mice groups (C26+CIS ANX-V % and C26 ANX-V %, respectively).

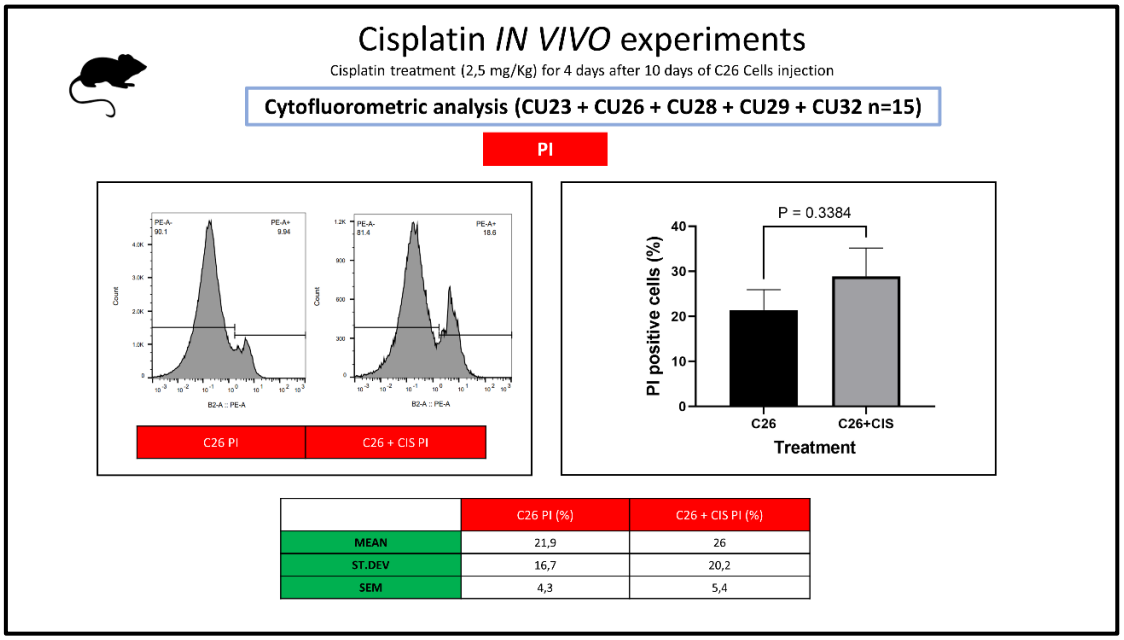

Figure 19. The figure shows the flow cytometry analysis of propidium iodide (PI) assay; the graph shows the comparison between the treated and untreated mice groups (C26+CIS and C26, respectively) in the percentage of propidium iodide (PI) positive cells. The table reports the mean values, standard deviation, and SEM of the percentage of propidium iodide (PI) positive cells in treated and untreated mice groups (C26+CIS PI % and C26 PI%, respectively).

In Vivo model: Statistical analysis

The statistical analysis was performed on five experiments, and every experiment was carried out in triplicate. As showed in figure 20A-B, we documented a high variability in standard deviation of data from both annexin-V and propidium iodide (PI) assay. The p-value of annexin-V data analysis reached a significant level in the fifth experiment, while the p-value of PI data analysis did not reach a significant level in 5 experiments although it showed a clear decreasing trend.

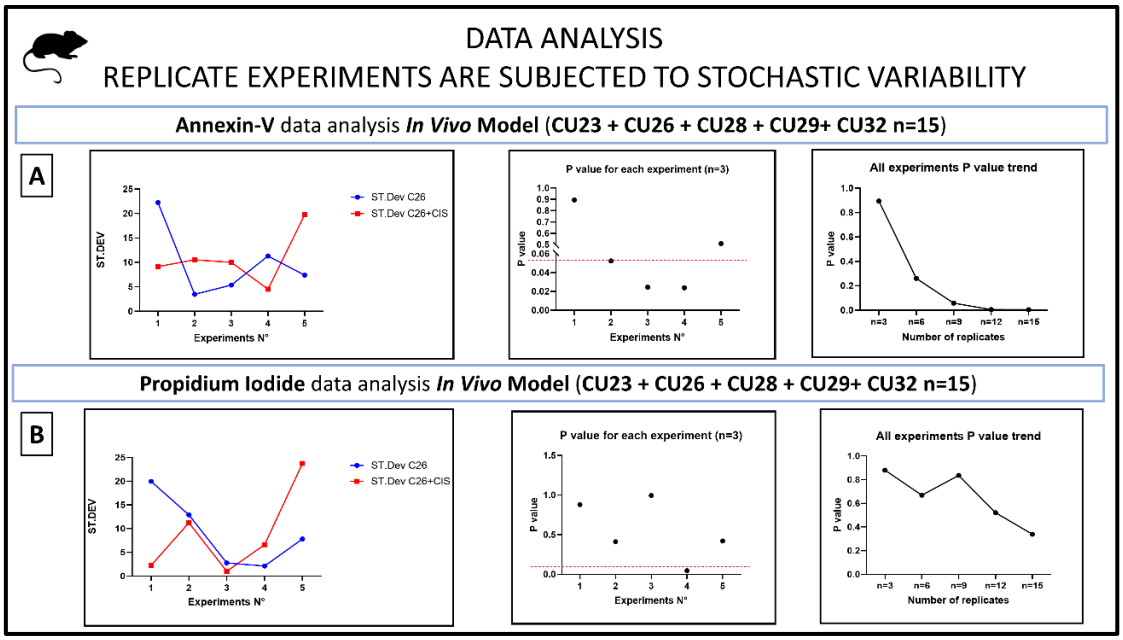

Figure 20. A) The figure shows the graphs reporting the standard deviation (ST.DEV), p values and p-value trend of five *in vivo* experiments evaluating the percentage of annexin-V positive cells in treated and untreated mice groups (C26=C26 untreated mice; C26+CIS=mice treated with cisplatin). **B)** The figure shows the graphs reporting the standard deviation (ST.DEV), p values, and p-value trend of five *in vivo* experiments evaluating the percentage of propidium iodide (PI) positive cells in treated and untreated mice groups (C26=C26 untreated mice; C26+CIS=mice treated with cisplatin).

In Vitro 3D-model: Characterizing 3D-model

As previously mentioned, C26 cells were cultured in a non-adherent surface (15ml falcon tube) allowing the cell-cell adhesion to produce tumor spheroids. Because of the novelty of this model we characterized the spheroids with hematoxylin-eosin staining to identify the diameter mean for aggregate(see figure 21) and, by the PI labeling we also described the percentage of dead cells per microscopic field (see figure 22).

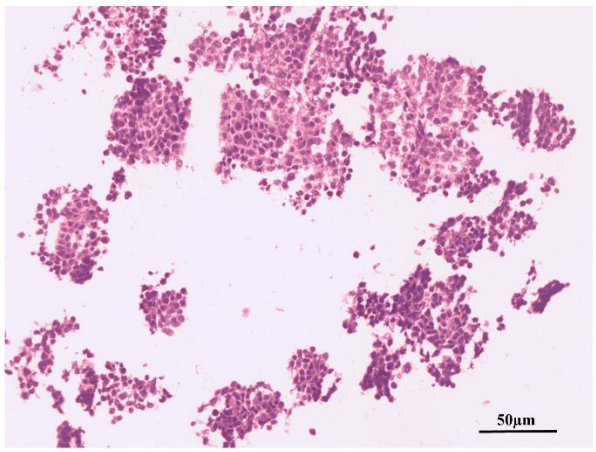

Experiment N°	Cells N°/ Aggregate	Diameter (µm) / Aggregate
#1	103	57
#2	87	37
#3	90	48
MEAN	93	47
ST.DEV	8,5	9,7

Figure 21. Hematoxylin/eosin staining of spheroids, magnification 10x. The table show the number of cells per aggregate and the mean of the diameters. The statistical analysis was carried out for 3 experiments in triplicates and the measurements were done using Image J software.

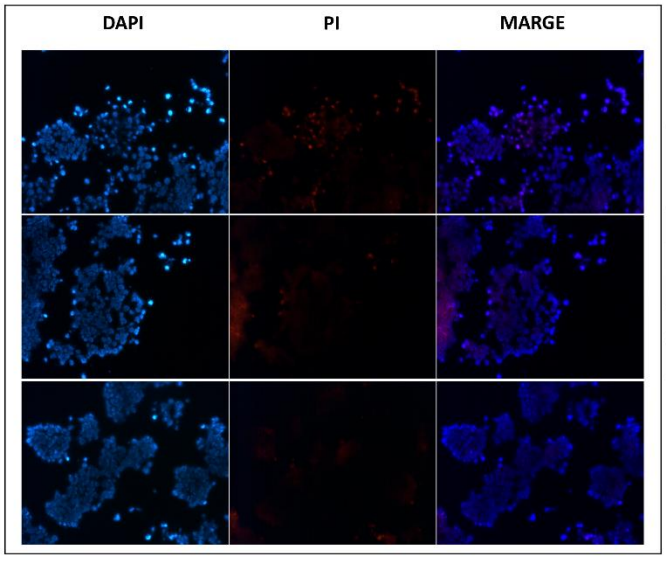

Experiment N°	Nuclei DAPI+	Nuclei PI+	PI+ Nuclei/ field Percentage (%)
#1	373	58	15,5
#2	324	29	8,8
#3	274	31	11,4
MEAN	323,7	39,3	12,1
ST.DEV	49,3	16,2	3,4

Figure 22. Propidium iodide/DAPI staining, magnification 10x. The statistical analysis was carried out for 3 experiments analyzing 3 microscopic fields per experiment. The table shows the percentage of PI (Propidium Iodide) positive cells in relation to the DAPI-stained cells per microscopic field.

In Vitro 3D-model: Targeting early and late apoptosis in cisplatin chemotherapy

Treatment with 1 µM Cisplatin performed on the 3D model, tumor-aggregates, did not seem to have induced early or late apoptotic processes. The flow cytometry data analysis reported in figure 23, show no statistically significant differences between the percentage of Annexin-V positive cells (early apoptotic cells) in both groups of tumor-aggregates.

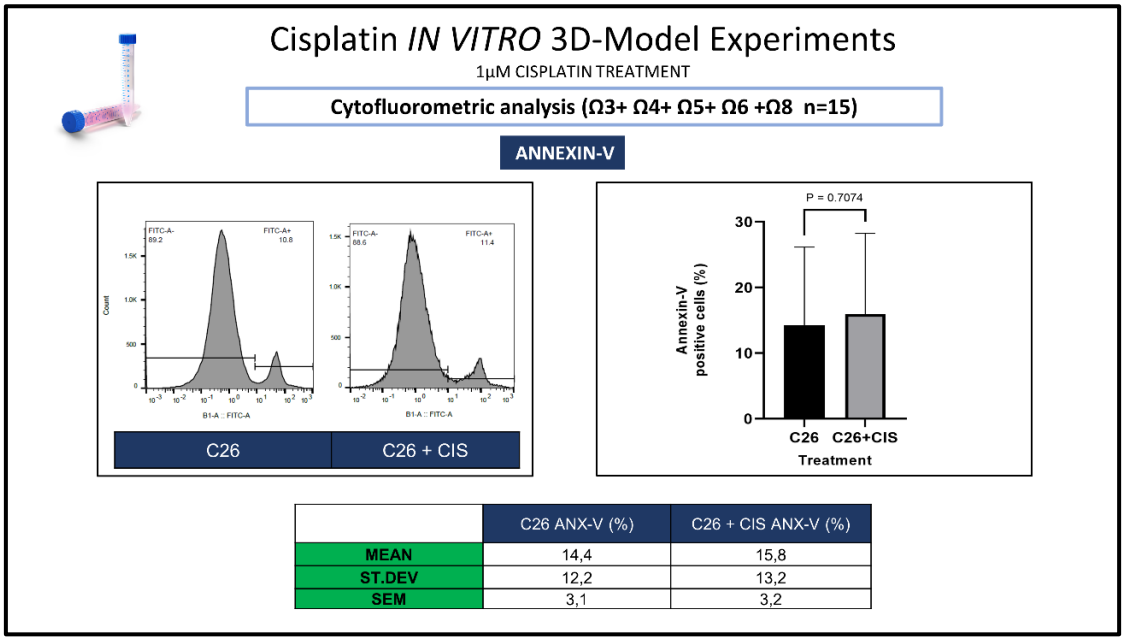

Figure 23. The figure shows the flow cytometry analysis of Annexin-V assay; the graph shows the comparison between the treated and untreated mice C26 cells (C26+CIS and C26, respectively) in percentage of annexin-V positive cells. The table reports the mean values, standard deviation, and SEM of the percentage of annexin-V positive cells in treated and untreated mice groups (C26+CIS ANX-V % and C26 ANX-V %, respectively).

Also the propidium iodide labelling documented no significant increase in the late-apoptotic/necrotic number of cells after the 1 µM cisplatin treatment in tumor-aggregates. The percentage of the PI positive cells in not-treated samples was similar to the treated condition (see figure 24).

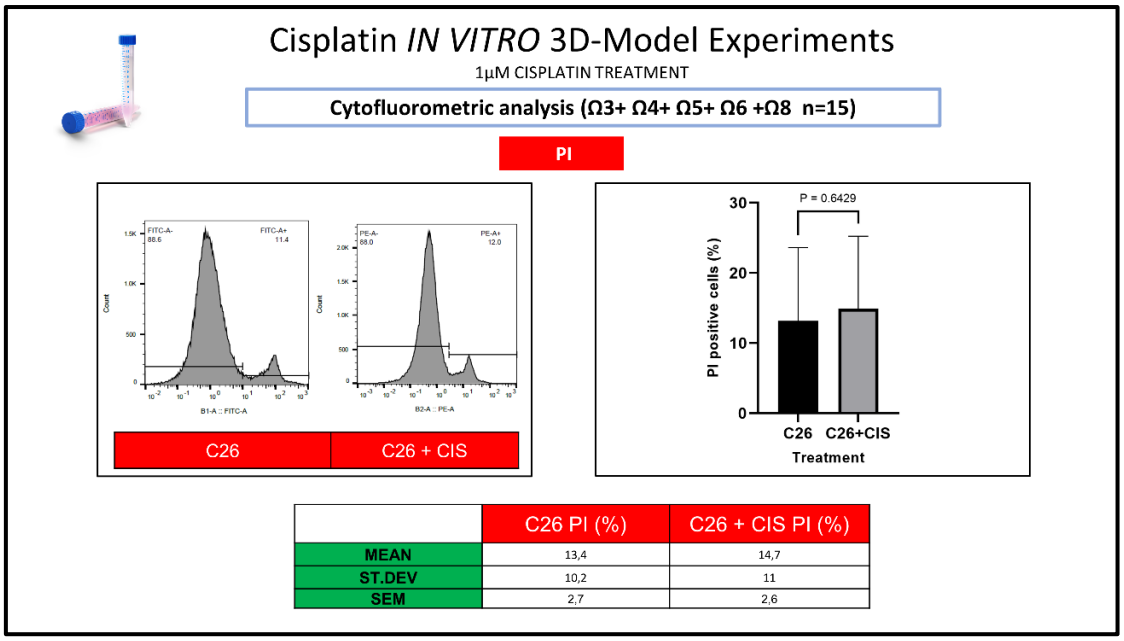

Figure 24. The figure shows the flow cytometry analysis of the propidium iodide (PI) assay; the graph shows the comparison between the treated and untreated C26 cells (C26+CIS and C26, respectively) in percentage of propidium iodide (PI) positive cells. The table reports the mean values, standard deviation, and SEM of the percentage of propidium iodide (PI) positive cells in treated and untreated mice groups (C26+CIS PI % and C26 PI%, respectively).

In Vitro 3D-model: Statistical analysis

The analysis of the distribution of the data collected during the 5 experiments reported values of standard deviation which vary during the experiments as well as the values of p.Unlike what was observed *in vivo* experiments, p values did not show a downward trend towards significant values increasing the number of the experiment (see figure 25).

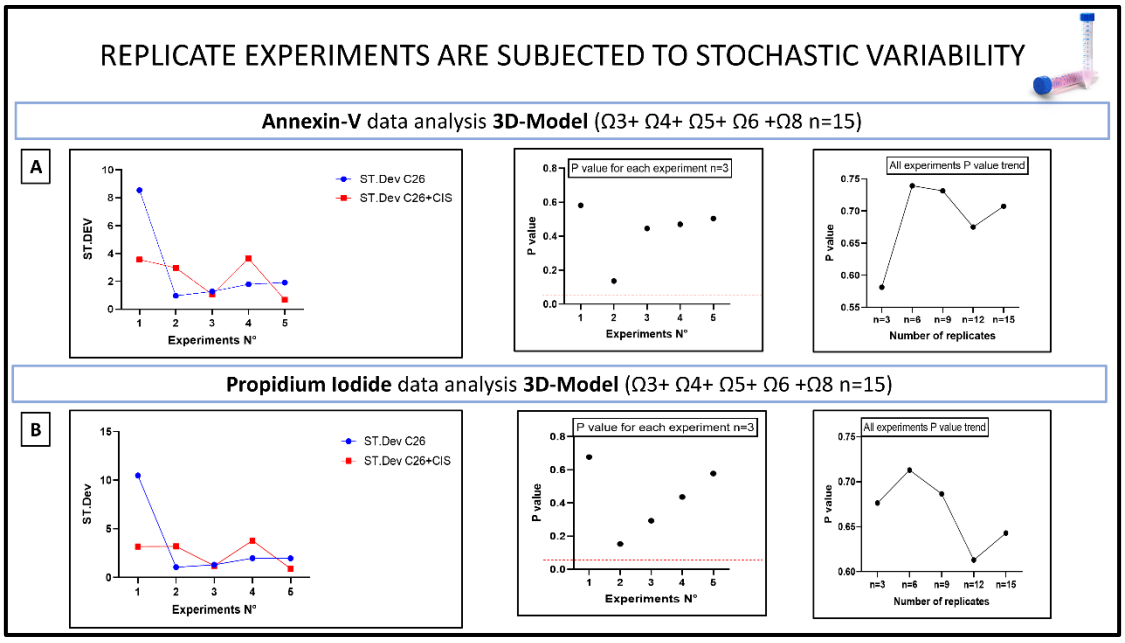

Figure 25. A) The figure shows the graphs reporting the standard deviation (ST.DEV), p values and p-value trend of five *in vitro* 3-D model experiments evaluating the percentage of annexin-V positive cells in treated and untreated mice groups (C26=C26 untreated mice; C26+CIS=mice treated with cisplatin). **B)** The figure shows the graphs reporting the standard deviation (ST.DEV), p values, and p-value trend of five *in vitro* 3-D model experiments evaluating the percentage of propidium iodide (PI) positive cells in treated and untreated mice groups (C26=C26 untreated mice; C26+CIS=mice treated with cisplatin).

Cisplatin *in vitro* experiments 2-D and 3D-model: Flow cytometric analysis of cell cycle with propidium iodide DNA staining

The preliminary results collected *in vitro* experiments (2D and 3D-model) showed a different cell distribution into the distinct phases of the cell cycle (see figure 26). However, the experiments are still ongoing and the new data could provide insight to elucidate the meaning of this different cellular behavior.

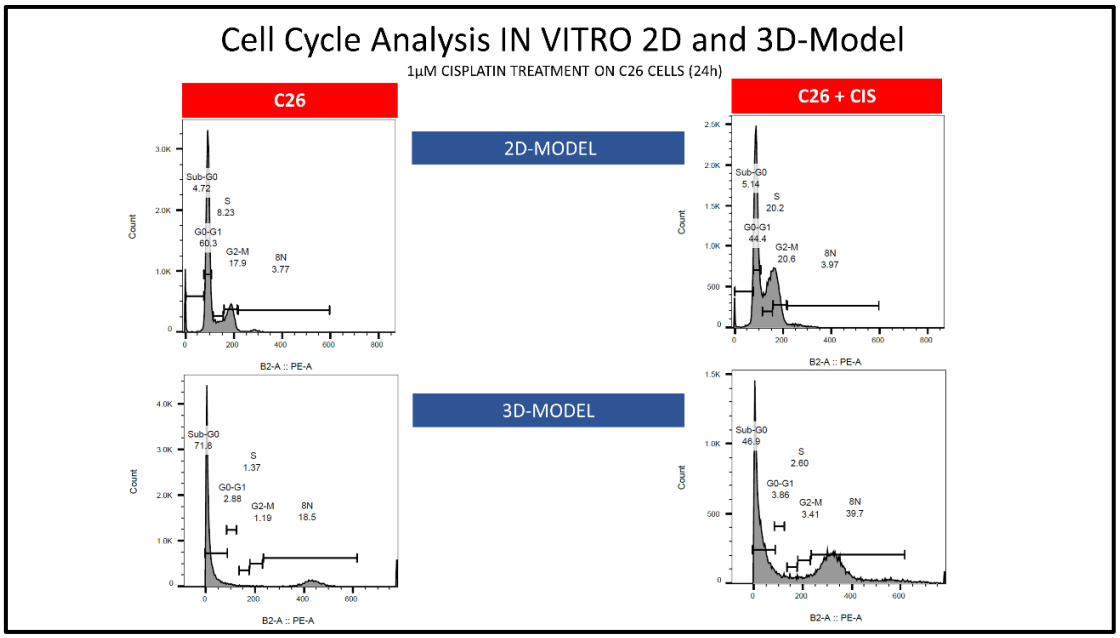

Figure 26. The figure reports the graphical analysis of the flow cytometry data obtained from the propidium iodide cell cycle assay. The graphs show a comparison between the 2D and 3D-model in cells distribution on the different phases of the cell cycle in relation to the cisplatin treatment. (C26= Untreated C26 cells; C26+CIS= Treated C26 cells).

Discussion

Despite ongoing advances and improvements in antitumor strategies, chemotherapy still holds the primary position as a cancer treatment method. Cisplatin, an effective genotoxic anticancer drug, works by inducing DNA damage and has been utilized in tumor treatment for several decades. However, genotoxic drugs have the disadvantage of being non-selective, requiring administration at high doses, which can cause toxicity in normal tissue(Li, M. et al., 2013). As a result, the issue of toxicity poses a significant challenge in the development of successful cancer chemotherapies.

In the present study, we proposed a chemotherapy treatment carried out by administering a lower dose of cisplatin compared with the cisplatin chemotherapy approaches described in scientific literature (Nowis, D. et al., 2008).

In particular, we reported the effects of chemotherapy treatment with 2.5 mg/kg of cisplatin in C26 tumor-bearing mice. The output measures of the efficacy of this treatment were the tumor weight and the weight loss of the mice. The mean of the tumors weights in the treated group of mice was 134.5 mg, while the untreated mice developed a mean tumor weight of 499 mg. This result suggests that at the dose of 2,5mg/Kg the cisplatin interferes with the tumor growth, reducing the tumor weight. Although the positive anti-cancer effect reported, we documented a significant impact of this treatment in body weight loss induction. The group of treated tumor-bearing mice showed a significant difference between the initial and the final body weight describing an increasing trend in body weight loss.

Conversely, the weight of the untreated mice did not change during the experiment. The initial body weight was recorded before the C26 cells inoculation and, after 15 days of tumor growth, the mice did not show any significant cachectic signs as documented by the comparison between initial and final body weight.

Since the well-known pro-cachectic effect of cisplatin chemotherapy, we studied the impact of the cisplatin 2,5 mg/Kg treatment on skeletal muscle. The comparison between the weight of the different skeletal muscles (anterior tibialis, gastrocnemius, extensor digitorum longus) did not reveal significant differences between the treated

and untreated groups. Interestingly, the comparison of the spleen weight, between the two groups showed a significant difference. The spleen weight of the mice untreated was significantly higher than the untreated counterpart. All these data together suggest that the dose of cisplatin (2,5 mg/Kg) used in these experiments was able to produce a strong effect in decreasing the tumor growth although it seems to trigger the cachexia-onset but still not involving the skeletal muscles, probably due to a low inflammation as suggested by the physiologic weight of the spleen. The increased weight loss that we documented could be interpreted basing on the scientific literature data. Garcia and colleagues (2013) hypnotized that cisplatin reduces de novo lipogenesis in all target organs (adipose tissue, liver and muscle). This reduction could be mainly attributed to the cisplatin-induced decrease in dietary intake, indeed decreases in the expression of lipogenic markers were observed when animals were treated with cisplatin compared to the control group. Furthermore, cisplatin has been shown to affect fat metabolism in the liver, in particular the enzyme stearoyl coenzyme A desaturase-1 (SCD-1), involved in the synthesis of monounsaturated fatty acids, was reduced by cisplatin. This decrease could promote fatty acid oxidation and reduce lipid synthesis in the liver.

However, the significant body weight loss observed in the treated mice has been taken into account to refine the cisplatin chemotherapy at a lower dose avoiding the risk to trigger the cachexia onset.

To face this crucial issue, and following the rationale of the 3Rs rule (Replace, Reduce, Refine)we planned a series of *in vitro* experiments aimed to propose a methodologic approach to the chemotherapy study.

Based on a cisplatin curve dose response *in vitro* model (C26 cell culture), as a preliminary result provided by our laboratory, we selected the lower dose of cisplatin presenting a borderline response in the anti-tumor effect. In particular, as the output of the anti-tumor effect, it was considered the number of DAPI-stained cells after 24 hours of 1µM cisplatin treatment compared to the not-treated C26 cells.

Considering the variable response to this low dose of cisplatin, we studied the treatment efficacy and the data dispersion during 5 experiments in triplicate (n=15). The results that we achieved, documented a significant impact of 1µM cisplatin treatment in decreasing the C26 cell culture proliferation.

Through the statistical analysis, we observed that the variability in sample data from every single experiment (n=3), demonstrated by high values of standard deviation, led to a not significant p-value. However, analyzing all together the data collected in 5 experiments (n=15) we identified a decreasing trend of the p values at a significant level.

To better clarify the mechanism of the cisplatin effect on tumor mass and C26 cell culture, we evaluated the processes of apoptosis and proliferation. Using two indicators of early and late apoptosis, Annexin-V and Propidium Iodide (PI) respectively, we documented the percentage of the cell damaged by the treatment.

In vivo model, the 4 days of cisplatin treatment (2,5 mg/Kg) induced a significant increase of the early apoptotic cell in the tumor mass while the amount of late-apoptotic/ necrotic cells did not undergo to significant change compared to the cell population from the tumor of untreated mice.

The same exploration has been performed *in vitro* 2D-model (C26 monolayer culture) by other colleagues of the research team. The preliminary data provided by these *in vitro* experiments documented the lack of response to a 1µM cisplatin treatment in increasing the amount of apoptotic/necrotic cell (early or late) although the significant reduction in number of cells highlighted with the microscopic analysis as above mentioned.

The monolayer cell cultures are very simplified models compared to the animal models and moreover with the human being. Thus, generalizing the data collected in these 2D-models is a hard issue to resolve. Accordingly with the 3Rs rationale, and in particular with the **R**eplace concept, we developed a 3D-model of multicellular tumor spheroids aimed to verify the cell behavior in response to the cisplatin chemotherapy.

The spheroids were characterized in their size, cell number content, and the physiologic ratio of live and dead cells. Subsequently, we tested the effect of 1µM cisplatin treatment on apoptosis. The data collected from the 3D-model were similar to the 2D-model data. Indeed the Annexin-V and PI labeling did not highlight a significant variation in apoptotic cell percentage between the two conditions (treated and untreated).

Comparing the data progression in replicate experiments in the 2D and 3D-model, we documented variability in data distribution between the triplicate samples in every experiment and also between the different experiments. In 2D-model experiments, we reported significant differences in the percentage of annexin-V positive cells only in one of five experiments, and analyzing all the data together (n=15) we detected a very slight decreasing trend of the p-value.

The PI analysis in 2D-model documented a significant effect of the cisplatin treatment in two of five experiments, and significant was also the analysis with a sample size of n=9 and n=12 although the analysis of all samples (n=15) did not reveal any significant differences in apoptosis induction between the treated and untreated conditions. As above mentioned for the annexin-V p values trend, in PI experiments we identified a stronger decreasing trend of the p values in relation to the sample size.

Conversely, the 1 μM cisplatin treatment *in vitro* 3-D model did not induce any significant increase of apoptotic (early or late) cell number as demonstrated by the annexin-V and PI assays. Interestingly, in both the analysis (annexin-V and PI) neither experiment reached a significant p-value and, moreover, there was not a clear trend of the p values in response to the increased sample size.

All these findings could be interpreted as a consequence of a different cisplatin availability between the two tumor-models studied. In a monolayer cell culture, every cell offers a surface of contact with the culture medium. Differently, the multicellular tumor spheroids are obtained after aggregation and compaction of cell suspension cultured in nonadherent conditions. Thus, the inner cells have indirect contact with the environment through the modulation of cell-cell interactions. Moreover, the multicellular tumor spheroids differ from another tumor 3D-model, the organotypic multicellular spheroids,because of the lack of cell heterogeneity. The organotypic multicellular spheroids are obtained from cutting tumor tissue and cultured in nonadherent conditions. This model is characterized by the presence of vascular structures, extracellular matrix, and different cell populations including fibroblasts and macrophages.(Bjerkvig, R. et al., 1990). Therefore, the presence of vascularization could be the reason of the different response to the cisplatin chemotherapy *in vivo* experiments compared to the multicellular tumor spheroids model.

Beside the evaluation of the pro-apoptotic effect of cisplatin chemotherapy, we also studied its impact on cellular proliferation as other process involved in tumor mass reduction. The primary mechanism of action of many cytotoxic agents involves DNA replication and the formation of mitotic spindles. Therefore, the analysis of the cell cycle could provide relevant advice of chemotherapy efficacy.

The preliminary results collected *in vitro* experiments (2D and 3D-model) showed a different cell behavior in response to the cisplatin treatment probably related to the cells culture architecture. In particular we found a different cell distribution into the distinct phases of the cell cycle.

In an animal model of orthotopic human gastric cancers, has been documented a phase specificity for the cisplatin chemotherapy activity. In particular, before the cisplatin treatment, 68% of the cells were in S, G2, or M phases while 32% were in G1/G0; after the treatment, 90% of the cells have been found in G1/G0 phase suggesting that cisplatin selectively targeted the actively proliferating cells(Yano S. et al., 2014).

Other studies, both *in vivo* and in a patient sample, documented a cell population blocked in G1 or G2/M phase after chemotherapy. These cells even if still viable seem to be unable to proliferate and they are considered in a senescence state (Michaloglou C. et al., 2005; Ewald J. et al., 2008; Ewald JA. Et al., 2010).

Interestingly, since 1993, it has been reported the induction of binucleated cells (BC) in cell culture after cisplatin treatment. The hypothesis proposed to explain the BC takes into account the blocking of cytokinesis or cell fusion. Moreover, *in vivo* and *in vitro* studies reported the formation of multinucleated cells with tripolar and tetrapolar mitosis together with the presence of fragmented DNA organized in micronuclei in the equatorial region of the cell(Rodilla V. 1993).

Considering the above mentioned studies our preliminary findings could be interpreted as blocking of cytokinesis resulting in aberrant cells with tripolar and tetrapolar mitosis after cisplatin treatment. However, the experiments are still ongoing and the new data could provide insight to elucidate the reason for this atypical cellular behavior.

Conclusion

The results obtained from both studies, although preliminary, have documented the efficacy of both approaches, pharmacological and non-pharmacological, in countering tumor growth by acting directly and indirectly on the tumor. Treatment with cisplatin, at a lower dosage than commonly reported in the scientific literature, significantly reduced tumor mass although it resulted in weight loss in the treated mice. However, the lack of muscle atrophy together with a normal spleen size suggests a reduction in the chemotherapy-related side effects.

Non-pharmacological treatment demonstrated that high-intensity exercise interfered with tumor growth mechanisms through the modulation of skeletal muscle secretory activity and the expression of ubiquitous proteins implicated in metabolic control and adaptation to stress. Previous studies have documented that cisplatin induces its side effects by increasing oxidative stress and pro-inflammatory cytokine release, both mechanisms targeted by exercise. In particular, exercise stimulates IL-6 secretion at the muscle level and reduces IL-1 and TNF-alpha levels, resulting in an anti-inflammatory environment. Additionally, exercise counteracts oxidative stress by inducing Hsp60 and Pgc1-alpha expression, optimizing fatty acid oxidation, and improving mitochondrial functions. A recent study on transgenic mice that constitutively express isoform 1 of PGC1-alpha (PGC1α-Tg1) showed that PGC1α-Tg1 mice maintained greater muscle mass and strength compared to control mice after cisplatin treatment, exhibiting higher exercise capacity and greater mitochondrial activity in skeletal muscles than control mice (Huot JR. et al., 2022).

Moreover, several studies demonstrated that Hsp60 may be involved in cisplatin resistance in some tumor cell lines (Kimura et al., 1993; Nakata et al., 1994; Hettinga et al., 1996; Abu-Hadid et al., 1997). Recently, a study by Harper et al., showed that inhibition of Hsp60 led to an increase in apoptosis of chemotherapy-resistant ovarian tumor cells suggesting that Hsp60 may represent a potential therapeutic target for increasing the effectiveness of chemotherapy in some neoplasms (Harper AK. et al., 2020). Therefore, the development of a therapeutic model that takes effect directly on

the tumor and simultaneously restores the general homeostasis of the organism seems to give relevant advantages, including a reduction in drugs resistance, increasing in their effectiveness, and the protection of organs from the non-selective action of chemotherapeutic agents.

References

Abu-Hadid M, Wilkes JD, Elakawi Z, Pendyala L, Perez RP. Relationship between heat shock protein 60 (HSP60) mRNA expression and resistance to platinum analogues in human ovarian and bladder carcinoma cell lines. Cancer Lett. 1997 Oct 28;119(1):63-70. doi: 10.1016/s0304-3835(97)00255-3. PMID: 18372523.

Achkar IW, Abdulrahman N, Al-Sulaiti H, Joseph JM, Uddin S, Mraiche F. Cisplatin based therapy: the role of the mitogen activated protein kinase signaling pathway. J Transl Med. 2018 Apr 11;16(1):96. doi: 10.1186/s12967-018-1471-1. PMID: 29642900; PMCID: PMC5896132.

Agrawal A, Suryakumar G, Rathor R. Role of defective Ca2+ signaling in skeletal muscle weakness: Pharmacological implications. J Cell Commun Signal. 2018 Dec;12(4):645-659. doi: 10.1007/s12079-018-0477-z. Epub 2018 Jul 7. PMID: 29982883; PMCID: PMC6235775.

Akerfelt M, Morimoto RI, Sistonen L. Heat shock factors: integrators of cell stress, development and lifespan. Nat Rev Mol Cell Biol. 2010 Aug;11(8):545-55. doi: 10.1038/nrm2938. Epub 2010 Jul 14. PMID: 20628411; PMCID: PMC3402356.

Amable L. Cisplatin resistance and opportunities for precision medicine. Pharmacol Res. 2016 Apr;106:27-36. doi: 10.1016/j.phrs.2016.01.001. Epub 2016 Jan 22. PMID: 26804248.

Amjad MT, Chidharla A, Kasi A. Cancer Chemotherapy. 2023 Feb 27. In: StatPearls [Internet]. Treasure Island (FL): StatPearls Publishing; 2023 Jan–. PMID: 33232037.

Arends J, Strasser F, Gonella S, Solheim TS, Madeddu C, Ravasco P, Buonaccorso L, de van der Schueren MAE, Baldwin C, Chasen M, Ripamonti CI; ESMO Guidelines Committee. Electronic address: clinicalguidelines@esmo.org. Cancer cachexia in adult patients: ESMO Clinical Practice Guidelines☆. ESMO Open. 2021 Jun;6(3):100092. doi: 10.1016/j.esmoop.2021.100092. PMID: 34144781; PMCID: PMC8233663.

Arita M, Watanabe S, Aoki N, Kuwahara S, Suzuki R, Goto S, Abe Y, Takahashi M, Sato M, Hokari S, Ohtsubo A, Shoji S, Nozaki K, Ichikawa K, Kondo R, Hayashi M, Ohshima Y, Kabasawa H, Hosojima M, Koya T, Saito A, Kikuchi T. Combination therapy of cisplatin with cilastatin enables an increased dose of cisplatin, enhancing its antitumor effect by suppression of nephrotoxicity. Sci Rep. 2021 Jan 12;11(1):750. doi: 10.1038/s41598-020-80853-6. PMID: 33437029; PMCID: PMC7804437.

Avan A, Postma TJ, Ceresa C, Avan A, Cavaletti G, Giovannetti E, Peters GJ. Platinum-induced neurotoxicity and preventive strategies: past, present, and future. Oncologist. 2015 Apr;20(4):411-32. doi: 10.1634/theoncologist.2014-0044. Epub 2015 Mar 12. PMID: 25765877; PMCID: PMC4391771.

Baar K. Involvement of PPAR gamma co-activator-1, nuclear respiratory factors 1 and 2, and PPAR alpha in the adaptive response to endurance exercise. Proc Nutr Soc. 2004 May;63(2):269-73. doi: 10.1079/PNS2004334. PMID: 15294042.

Balkwill F. (2006). TNF-alpha in promotion and progression of cancer. Cancer metastasis reviews, 25(3), 409–416. https://doi.org/10.1007/s10555-006-9005-3

Balkwill, F., & Mantovani, A. (2001). Inflammation and cancer: back to Virchow?. Lancet (London, England), 357(9255), 539–545. https://doi.org/10.1016/S0140-6736(00)04046-0

Baracos, V.E.; Martin, L.; Korc, M.; Guttridge D.C.; Fearon, K.C.H. Cancer-associated cachexia. Nat Rev Dis Primers. 2018, 18, 4,17105; DOI: 10.1038/nrdp.2017.105.

Barone R, Macaluso F, Sangiorgi C, Campanella C, Marino Gammazza A, Moresi V, Coletti D, Conway de Macario E, Macario AJ, Cappello F, Adamo S, Farina F, Zummo G, Di Felice V. Skeletal muscle Heat shock protein 60 increases after endurance training and induces peroxisome proliferator-activated receptor gamma coactivator 1 α1 expression. Sci Rep. 2016 Jan 27;6:19781. doi: 10.1038/srep19781. PMID: 26812922; PMCID: PMC4728392.

Basu A, Ghosh P, Bhattacharjee A, Patra AR, Bhattacharya S. Prevention of myelosuppression and genotoxicity induced by cisplatin in murine bone marrow cells: effect of an organovanadium compound vanadium(III)-l-cysteine. Mutagenesis. 2015 Jul;30(4):509-17. doi: 10.1093/mutage/gev011. Epub 2015 Mar 16. PMID: 25778689; PMCID: PMC5943823.

Behmand, B., Noronha, A. M., Wilds, C. J., Marignier, J. L., Mostafavi, M., Wagner, J. R., Hunting, D. J., & Sanche, L. (2020). Hydrated electrons induce the formation of interstrand cross-links in DNA modified by cisplatin adducts. Journal of radiation research, 61(3), 343–351. https://doi.org/10.1093/jrr/rraa014.

Bjerkvig R, Tønnesen A, Laerum OD, Backlund EO. Multicellular tumor spheroids from human gliomas maintained in organ culture. J Neurosurg. 1990 Mar;72(3):463-75. doi: 10.3171/jns.1990.72.3.0463. PMID: 2406382.

Bordignon C, Dos Santos BS, Rosa DD. Impact of Cancer Cachexia on Cardiac and Skeletal Muscle: Role of Exercise Training. Cancers (Basel). 2022 Jan 11;14(2):342. doi: 10.3390/cancers14020342. PMID: 35053505; PMCID: PMC8773522.

Bost F, Kaminski L. The metabolic modulator PGC-1α in cancer. Am J Cancer Res. 2019 Feb 1;9(2):198-211. PMID: 30906622; PMCID: PMC6405967.

Boutilier AJ, Elsawa SF. Macrophage Polarization States in the Tumor Microenvironment. Int J Mol Sci. 2021 Jun 29;22(13):6995. doi: 10.3390/ijms22136995. PMID: 34209703; PMCID: PMC8268869.

Brierley DI, Harman JR, Giallourou N, Leishman E, Roashan AE, Mellows BAD, Bradshaw HB, Swann JR, Patel K, Whalley BJ, Williams CM. Chemotherapy-induced cachexia dysregulates hypothalamic and systemic lipoamines and is attenuated by cannabigerol. J Cachexia Sarcopenia Muscle. 2019 Aug;10(4):844-859. doi: 10.1002/jcsm.12426. Epub 2019 Apr 29. PMID: 31035309; PMCID: PMC6711413.

Brown JL, Lawrence MM, Ahn B, Kneis P, Piekarz KM, Qaisar R, Ranjit R, Bian J, Pharaoh G, Brown C, Peelor FF 3rd, Kinter MT, Miller BF, Richardson A, Van Remmen H. Cancer cachexia in a mouse model of oxidative stress. J Cachexia Sarcopenia Muscle. 2020 Dec;11(6):1688-1704. doi: 10.1002/jcsm.12615. Epub 2020 Sep 12. PMID: 32918528; PMCID: PMC7749559.

Bukau B, Weissman J, Horwich A. Molecular chaperones and protein quality control. Cell. 2006 May 5;125(3):443-51. doi: 10.1016/j.cell.2006.04.014. PMID: 16678092.

Cappello F, Angileri F, de Macario EC, Macario AJ. Chaperonopathies and chaperonotherapy. Hsp60 as therapeutic target in cancer: potential benefits and risks. Curr Pharm Des. 2013;19(3):452-7. PMID: 22920896.
Cappello F, Angileri F, de Macario EC, Macario AJ. Chaperonopathies and chaperonotherapy. Hsp60 as therapeutic target in cancer: potential benefits and risks. Curr Pharm Des. 2013;19(3):452-7. PMID: 22920896.

Cappello F, David S, Peri G, Farina F, Conway de Macario E, Macario AJ, Zummo G. Hsp60: molecular anatomy and role in colorectal cancer diagnosis and treatment. Front Biosci (Schol Ed). 2011 Jan 1;3(1):341-51. doi: 10.2741/s155. PMID: 21196380.

Cappello F, Marino Gammazza A, Palumbo Piccionello A, Campanella C, Pace A, Conway de Macario E, Macario AJ. Hsp60 chaperonopathies and chaperonotherapy: targets and agents. Expert Opin Ther Targets. 2014 Feb;18(2):185-208. doi: 10.1517/14728222.2014.856417. Epub 2013 Nov 29. PMID: 24286280.

Caruso Bavisotto C, Alberti G, Vitale AM, Paladino L, Campanella C, Rappa F, Gorska M, Conway de Macario E, Cappello F, Macario AJL, Marino Gammazza A.

Hsp60 Post-translational Modifications: Functional and Pathological Consequences. Front Mol Biosci. 2020 Jun 4;7:95. doi: 10.3389/fmolb.2020.00095. PMID: 32582761; PMCID: PMC7289027.

Christensen JF, Simonsen C, Hojman P. Exercise Training in Cancer Control and Treatment. Compr Physiol. 2018 Dec 13;9(1):165-205. doi: 10.1002/cphy.c180016. PMID: 30549018.

Cömert C, Fernandez-Guerra P, Bross P. A Cell Model for HSP60 Deficiencies: Modeling Different Levels of Chaperonopathies Leading to Oxidative Stress and Mitochondrial Dysfunction. Methods Mol Biol. 2019;1873:225-239. doi: 10.1007/978-1-4939-8820-4_14. PMID: 30341613.

Conte E, Bresciani E, Rizzi L, Cappellari O, De Luca A, Torsello A, Liantonio A. Cisplatin-InducedSkeletal Muscle Dysfunction: Mechanisms and CounteractingTherapeutic Strategies. Int J Mol Sci. 2020 Feb 13;21(4):1242. doi: 10.3390/ijms21041242. PMID: 32069876; PMCID: PMC7072891.

Coussens LM, Werb Z. Inflammation and cancer. Nature. 2002 Dec 19-26;420(6917):860-7. doi: 10.1038/nature01322. PMID: 12490959; PMCID: PMC2803035.

D'Amico D, Fiore R, Caporossi D, Di Felice VD, Cappello F, Dimauro I, Barone R. Function and Fiber-Type Specific Distribution of Hsp60 and αB-Crystallin in Skeletal Muscles: Role of Physical Exercise. Biology (Basel). 2021 Jan 21;10(2):77. doi: 10.3390/biology10020077. PMID: 33494467; PMCID: PMC7911561.

D'Amico D, Marino Gammazza A, Macaluso F, Paladino L, Scalia F, Spinoso G, Dimauro I, Caporossi D, Cappello F, Di Felice V, Barone R. Sex-based differences after a single bout of exercise on PGC1α isoforms in skeletal muscle: A pilot study. FASEB J. 2021 Feb;35(2):e21328. doi: 10.1096/fj.202002173R. PMID: 33433932.

Damrauer JS, Stadler ME, Acharyya S, Baldwin AS, Couch ME, Guttridge DC. Chemotherapy-induced muscle wasting: association with NF-κB and cancer cachexia. Eur J Transl Myol. 2018 Jun 6;28(2):7590. doi: 10.4081/ejtm.2018.7590. PMID: 29991992; PMCID: PMC6036305.

Damrauer JS, Stadler ME, Acharyya S, Baldwin AS, Couch ME, Guttridge DC. Chemotherapy-induced muscle wasting: association with NF-κB and cancer cachexia. Eur J Transl Myol. 2018 Jun 6;28(2):7590. doi: 10.4081/ejtm.2018.7590. PMID: 29991992; PMCID: PMC6036305.

Daou HN. Exercise as an anti-inflammatory therapy for cancer cachexia: a focus on interleukin-6 regulation. Am J Physiol Regul Integr Comp Physiol. 2020 Feb 1;318(2):R296-R310. doi: 10.1152/ajpregu.00147.2019. Epub 2019 Dec 11. PMID: 31823669.

Dasari, S., & Tchounwou, P. B. (2014). Cisplatin in cancer therapy: molecular mechanisms of action. European journal of pharmacology, 740, 364–378. https://doi.org/10.1016/j.ejphar.2014.07.025.

Delgado JL, Hsieh CM, Chan NL, Hiasa H. Topoisomerases as anticancer targets. Biochem J. 2018 Jan 23;475(2):373-398. doi: 10.1042/BCJ20160583. PMID: 29363591; PMCID: PMC6110615.

Dev, R.; Hui, D.; Chisholm, G.; Delgado-Guay, M.; Dalal, S., Del Fabbro, E.; Bruera, E. Hypermetabolism and symptom burden in advanced cancer patients evaluated in a cachexia clinic. Journal of cachexia, sarcopenia and muscle. 2015, 6, 95–98.

Dieli-Conwright, C. M., Courneya, K. S., Demark-Wahnefried, W., Sami, N., Lee, K., Sweeney, F. C., Stewart, C., Buchanan, T. A., Spicer, D., Tripathy, D., Bernstein, L., & Mortimer, J. E. (2018). Aerobic and resistance exercise improves physical fitness, bone health, and quality of life in overweight and obese breast cancer survivors: a randomized controlled trial. Breast cancer research : BCR, 20(1), 124. https://doi.org/10.1186/s13058-018-1051-6

Ellis H. (2015). Paul Ehrlich: Nobel laureate and father of modern chemotherapy. British journal of hospital medicine (London, England : 2005), 76(8), 483. https://doi.org/10.12968/hmed.2015.76.8.483

Evans, W.J.; Morley, J.E.; Argilés, J.; Bales, C.; Baracos, V.E.; Guttridge, D.; Jatoi, A.; Kalantar-Zadeh, K.; Lochs, H.; Mantovani, G.; et al. Cachexia: a new definition. Clin Nutr. 2008, 27, 793-799; DOI: 10.1016/j.clnu.2008.06.013.

Ewald J, Desotelle J, Almassi N, Jarrard D. Drug-induced senescence bystander proliferation in prostate cancer cells in vitro and in vivo. Br J Cancer. 2008 Apr 8;98(7):1244-9. doi: 10.1038/sj.bjc.6604288. Epub 2008 Mar 18. PMID: 18349844; PMCID: PMC2359629.

Ewald JA, Desotelle JA, Wilding G, Jarrard DF. Therapy-induced senescence in cancer. J Natl Cancer Inst. 2010 Oct 20;102(20):1536-46. doi: 10.1093/jnci/djq364. Epub 2010 Sep 21. PMID: 20858887; PMCID: PMC2957429.

Fearon, K.; Strasser, F.; Anker, S.D.; Bosaeus, I.; Bruera, E.; Fainsinger, R.L.; Jatoi, A.; Loprinzi, C.; MacDonald, N.; Mantovani, G.; et al. Definition and classification of cancer cachexia: an international consensus. Lancet Oncol. 2011, 12, 489-495; DOI: 10.1016/S1470-2045(10)70218-7.

Folkesson M., Mackey A.L., Langberg H., Oskarsson E., Piehl-Aulin K., Henriksson J., Kadi F. The expression of heat shock protein in human skeletal muscle: Effects of muscle fibre phenotype and training background. Acta Physiol. 2013;209:26–33. doi: 10.1111/apha.12124.

Fonseca GWPD, Farkas J, Dora E, von Haehling S, Lainscak M. Cancer Cachexia and Related Metabolic Dysfunction. Int J Mol Sci. 2020 Mar 27;21(7):2321. doi: 10.3390/ijms21072321. PMID: 32230855; PMCID: PMC7177950.

Galluzzi, L., Senovilla, L., Vitale, I., Michels, J., Martins, I., Kepp, O., Castedo, M., &Kroemer, G. (2012). Molecular mechanisms of cisplatin resistance. Oncogene, 31(15), 1869–1883. https://doi.org/10.1038/onc.2011.384.

Garcia JM, Scherer T, Chen JA, Guillory B, Nassif A, Papusha V, Smiechowska J, Asnicar M, Buettner C, Smith RG. Inhibition of cisplatin-induced lipid catabolism and weight loss by ghrelin in male mice. Endocrinology. 2013 Sep;154(9):3118-29. doi: 10.1210/en.2013-1179. Epub 2013 Jul 5. PMID: 23832960; PMCID: PMC3749475.

Gupta RS. Evolution of the chaperonin families (Hsp60, Hsp10 and Tcp-1) of proteins and the origin of eukaryotic cells. Mol Microbiol. 1995 Jan;15(1):1-11. doi: 10.1111/j.1365-2958.1995.tb02216.x. PMID: 7752884.

Gupta SC, Hevia D, Patchva S, Park B, Koh W, Aggarwal BB. Upsides and downsides of reactive oxygen species for cancer: the roles of reactive oxygen species in tumorigenesis, prevention, and therapy. Antioxid Redox Signal. 2012 Jun 1;16(11):1295-322. doi: 10.1089/ars.2011.4414. Epub 2012 Jan 16. PMID: 22117137; PMCID: PMC3324815.

Hagymasi AT, Dempsey JP, Srivastava PK. Heat-Shock Proteins. Curr Protoc. 2022 Nov;2(11):e592. doi: 10.1002/cpz1.592. PMID: 36367390.

Harper AK, Fletcher NM, Fan R, Morris RT, Saed GM. Heat Shock Protein 60 (HSP60) Serves as a Potential Target for the Sensitization of Chemoresistant Ovarian Cancer Cells. Reprod Sci. 2020 Apr;27(4):1030-1036. doi: 10.1007/s43032-019-00089-2. Epub 2020 Mar 2. PMID: 32124395.

Hartl FU, Hayer-Hartl M. Molecular chaperones in the cytosol: from nascent chain to folded protein. Science. 2002 Mar 8;295(5561):1852-8. doi: 10.1126/science.1068408. PMID: 11884745.

Hayati F, Hossainzadeh M, Shayanpour S, Abedi-Gheshlaghi Z, Beladi Mousavi SS. Prevention of cisplatin nephrotoxicity. J Nephropharmacol. 2015 Aug 22;5(1):57-60. PMID: 28197500; PMCID: PMC5297508.

He C, Sun Z, Hoffman RM, Yang Z, Jiang Y, Wang L, Hao Y. P-Glycoprotein Overexpression Is Associated With Cisplatin Resistance in Human Osteosarcoma. Anticancer Res. 2019 Apr;39(4):1711-1718. doi: 10.21873/anticanres.13277. PMID: 30952710.

Hettinga JV, Lemstra W, Meijer C, Los G, de Vries EG, Konings AW, Kampinga HH. Heat-shock protein expression in cisplatin-sensitive and -resistant human tumor cells. Int J Cancer. 1996 Sep 17;67(6):800-7. doi: 10.1002/(SICI)1097-0215(19960917)67:6<800::AID-IJC8>3.0.CO;2-V. PMID: 8824551.

Hojman P, Gehl J, Christensen JF, Pedersen BK. Molecular Mechanisms Linking Exercise to Cancer Prevention and Treatment. Cell Metab. 2018 Jan 9;27(1):10-21. doi: 10.1016/j.cmet.2017.09.015. Epub 2017 Oct 19. PMID: 29056514.

Huot JR, Pin F, Chatterjee R, Bonetto A. PGC1α overexpression preserves muscle mass and function in cisplatin-induced cachexia. J Cachexia Sarcopenia Muscle. 2022 Oct;13(5):2480-2491. doi: 10.1002/jcsm.13035. Epub 2022 Jul 28. PMID: 35903870; PMCID: PMC9530502.

Huot JR, Pin F, Chatterjee R, Bonetto A. PGC1α overexpression preserves muscle mass and function in cisplatin-induced cachexia. J Cachexia Sarcopenia Muscle. 2022 Oct;13(5):2480-2491. doi: 10.1002/jcsm.13035. Epub 2022 Jul 28. PMID: 35903870; PMCID: PMC9530502.

Igarashi J, Okamoto R, Yamashita T, Hashimoto T, Karita S, Nakai K, Kubota Y, Takata M, Yamaguchi F, Tokuda M, Sakakibara N, Tsukamoto I, Konishi R, Hirano K. A key role of PGC-1α transcriptional coactivator in production of VEGF by a novel angiogenic agent COA-Cl in cultured human fibroblasts. Physiol Rep. 2016 Mar;4(6):e12742. doi: 10.14814/phy2.12742. Epub 2016 Mar 31. PMID: 27033444; PMCID: PMC4814893.

Irwin, M. L., Smith, A. W., McTiernan, A., Ballard-Barbash, R., Cronin, K., Gilliland, F. D., Baumgartner, R. N., Baumgartner, K. B., & Bernstein, L. (2008). Influence of pre- and postdiagnosis physical activity on mortality in breast cancer survivors: the health, eating, activity, and lifestyle study. Journal of clinical oncology : official journal of the American Society of Clinical Oncology, 26(24), 3958–3964. https://doi.org/10.1200/JCO.2007.15.9822.

Javid H, Hashemian P, Yazdani S, Sharbaf Mashhad A, Karimi-Shahri M. The role of heat shock proteins in metastatic colorectal cancer: A review. J Cell Biochem. 2022 Nov;123(11):1704-1735. doi: 10.1002/jcb.30326. Epub 2022 Sep 5. PMID: 36063530.

Jee H. Size dependent classification of heat shock proteins: a mini-review. J Exerc Rehabil. 2016 Aug 31;12(4):255-9. doi: 10.12965/jer.1632642.321. PMID: 27656620; PMCID: PMC5031383.

Kanat O, Ertas H, Caner B. Platinum-induced neurotoxicity: A review of possible mechanisms. World J Clin Oncol. 2017 Aug 10;8(4):329-335. doi: 10.5306/wjco.v8.i4.329. PMID: 28848699; PMCID: PMC5554876.

Karati D, Mahadik KR, Trivedi P, Kumar D. Alkylating Agents, the Road Less Traversed, Changing Anticancer Therapy. Anticancer Agents Med Chem. 2022;22(8):1478-1495. doi: 10.2174/1871520621666210811105344. PMID: 34382529.

Kasvis P, Vigano M, Vigano A. Health-related quality of life across cancer cachexia stages. Ann Palliat Med. 2019 Jan;8(1):33-42. doi: 10.21037/apm.2018.08.04. Epub 2018 Sep 5. PMID: 30525763.

Khosravi N, Stoner L, Farajivafa V, Hanson ED. Exercise training, circulating cytokine levels and immune function in cancer survivors: A meta-analysis. Brain Behav Immun. 2019 Oct;81:92-104. doi: 10.1016/j.bbi.2019.08.187. Epub 2019 Aug 24. PMID: 31454519.

Kim GT, Kim EY, Shin SH, Lee H, Lee SH, Park K, Sohn KY, Yoon SY, Kim JW. PLAG alleviates cisplatin-induced cachexia in lung cancer implanted mice. Transl Oncol. 2022 Jun;20:101398. doi: 10.1016/j.tranon.2022.101398. Epub 2022 Mar 24. PMID: 35339890; PMCID: PMC8957043.

Kimura E, Enns RE, Thiebaut F, Howell SB. Regulation of HSP60 mRNA expression in a human ovarian carcinoma cell line. Cancer Chemother Pharmacol. 1993;32(4):279-85. doi: 10.1007/BF00686173. PMID: 8100743.

Kneis S, Wehrle A, Müller J, Maurer C, Ihorst G, Gollhofer A, Bertz H. It's never too late - balance and endurance training improves functional performance, quality of life, and alleviates neuropathic symptoms in cancer survivors suffering from chemotherapy-induced peripheral neuropathy: results of a randomized controlled trial. BMC Cancer. 2019 May 2;19(1):414. doi: 10.1186/s12885-019-5522-7. PMID: 31046719; PMCID: PMC6498676.

Knudsen NH, Stanya KJ, Hyde AL, Chalom MM, Alexander RK, Liou YH, Starost KA, Gangl MR, Jacobi D, Liu S, Sopariwala DH, Fonseca-Pereira D, Li J, Hu FB, Garrett WS, Narkar VA, Ortlund EA, Kim JH, Paton CM, Cooper JA, Lee CH. Interleukin-13 drives metabolic conditioning of muscle to endurance exercise. Science. 2020 May 1;368(6490):eaat3987. doi: 10.1126/science.aat3987. Epub 2020 Apr 30. PMID: 32355002; PMCID: PMC7549736.

Köberle B, Schoch S. Platinum Complexes in Colorectal Cancer and Other Solid Tumors. Cancers (Basel). 2021 Apr 25;13(9):2073. doi: 10.3390/cancers13092073. PMID: 33922989; PMCID: PMC8123298.

Law ML. Cancer cachexia: Pathophysiology and association with cancer-related pain. Front Pain Res (Lausanne). 2022 Aug 22;3:971295. doi: 10.3389/fpain.2022.971295. PMID: 36072367; PMCID: PMC9441771.

Li M, Wang J, Tan SY, Chen JH, Cui W, Chen ZQ, Zhang J. Growth inhibition effect of peptide P110 plus cisplatin on various cancer cells and xenotransplanted tumors in mice. Mol Med Rep. 2013 Apr;7(4):1149-54. doi: 10.3892/mmr.2013.1343. Epub 2013 Feb 26. PMID: 23447049.

Lin J, Wu H, Tarr PT, Zhang CY, Wu Z, Boss O, Michael LF, Puigserver P, Isotani E, Olson EN, Lowell BB, Bassel-Duby R, Spiegelman BM. Transcriptional co-activator PGC-1 alpha drives the formation of slow-twitch muscle fibres. Nature. 2002 Aug 15;418(6899):797-801. doi: 10.1038/nature00904. PMID: 12181572.

Macario AJ, Conway de Macario E. Chaperonopathies and chaperonotherapy. FEBS Lett. 2007 Jul 31;581(19):3681-8. doi: 10.1016/j.febslet.2007.04.030. Epub 2007 Apr 24. PMID: 17475257.

Magnano, S., HannonBarroeta, P., Duffy, R., O'Sullivan, J., &Zisterer, D. M. (2021). Cisplatin induces autophagy-associated apoptosis in human oral squamous cell carcinoma (OSCC) mediated in part through reactive oxygen species. Toxicology and applied pharmacology, 427, 115646. https://doi.org/10.1016/j.taap.2021.115646.

Mangano, G. D., Fouani, M., D'Amico, D., Di Felice, V., & Barone, R. (2022). Cancer-Related Cachexia: The Vicious Circle between Inflammatory Cytokines, Skeletal Muscle, Lipid Metabolism and the Possible Role of Physical Training. International journal of molecular sciences, 23(6), 3004. https://doi.org/10.3390/ijms23063004.

Marino Gammazza A, Macaluso F, Di Felice V, Cappello F, Barone R. Hsp60 in Skeletal Muscle Fiber Biogenesis and Homeostasis: From Physical Exercise to Skeletal Muscle Pathology. Cells. 2018 Nov 22;7(12):224. doi: 10.3390/cells7120224. PMID: 30469470; PMCID: PMC6315887.

Martin A, Freyssenet D. Phenotypic features of cancer cachexia-related loss of skeletal muscle mass and function: lessons from human and animal studies. J Cachexia Sarcopenia Muscle. 2021 Apr;12(2):252-273. doi: 10.1002/jcsm.12678. Epub 2021 Mar 30. PMID: 33783983; PMCID: PMC8061402.

Martínez-Redondo V, Pettersson AT, Ruas JL. The hitchhiker's guide to PGC-1α isoform structure and biological functions. Diabetologia. 2015 Sep;58(9):1969-77. doi: 10.1007/s00125-015-3671-z. Epub 2015 Jun 25. PMID: 26109214.

McSweeney KR, Gadanec LK, Qaradakhi T, Ali BA, Zulli A, Apostolopoulos V. Mechanisms of Cisplatin-Induced Acute Kidney Injury: Pathological Mechanisms, Pharmacological Interventions, and Genetic Mitigations. Cancers (Basel). 2021 Mar 29;13(7):1572. doi: 10.3390/cancers13071572. PMID: 33805488; PMCID: PMC8036620.

Metsios, G. S., Moe, R. H., & Kitas, G. D. (2020). Exercise and inflammation. Best practice & research. Clinical rheumatology, 34(2), 101504. https://doi.org/10.1016/j.berh.2020.101504

Michaloglou C, Vredeveld LC, Soengas MS, Denoyelle C, Kuilman T, van der Horst CM, Majoor DM, Shay JW, Mooi WJ, Peeper DS. BRAFE600-associated senescence-like cell cycle arrest of human naevi. Nature. 2005 Aug 4;436(7051):720-4. doi: 10.1038/nature03890. PMID: 16079850.

Mok J, Brown MJ, Akam EC, Morris MA. The lasting effects of resistance and endurance exercise interventions on breast cancer patient mental well-being and physical fitness. Sci Rep. 2022 Mar 3;12(1):3504. doi: 10.1038/s41598-022-07446-3. PMID: 35241723; PMCID: PMC8894392.

Moreira-Pais A, Ferreira R, Gil da Costa R. Platinum-induced muscle wasting in cancer chemotherapy: Mechanisms and potential targets for therapeutic intervention. Life Sci. 2018 Sep 1;208:1-9. doi: 10.1016/j.lfs.2018.07.010. Epub 2018 Jul 6. PMID: 30146014.

Morton JP, Maclaren DP, Cable NT, Campbell IT, Evans L, Kayani AC, McArdle A, Drust B. Trained men display increased basal heat shock protein content of

skeletal muscle. Med Sci Sports Exerc. 2008 Jul;40(7):1255-62. doi:10.1249/MSS.0b013e31816a7171. PMID: 18580405.

Muoio DM, Koves TR. Skeletal muscle adaptation to fatty acid depends on coordinated actions of the PPARs and PGC1 alpha: implications for metabolic disease. Appl Physiol Nutr Metab. 2007 Oct;32(5):874-83. doi: 10.1139/H07-083. PMID: 18059612.

Nakata B, Barton R, Robbins K, Howell S, Los G. Association between hsp60 messenger-RNA levels and Cisplatin resistance in human head and neck-cancer cell-lines. Int J Oncol. 1994 Dec;5(6):1425-32. doi: 10.3892/ijo.5.6.1425. PMID: 21559731.

Nowis D, Bugajski M, Winiarska M, Bil J, Szokalska A, Salwa P, Issat T, Was H, Jozkowicz A, Dulak J, Stoklosa T, Golab J. Zinc protoporphyrin IX, a heme oxygenase-1 inhibitor, demonstrates potent antitumor effects but is unable to potentiate antitumor effects of chemotherapeutics in mice. BMC Cancer. 2008 Jul 11;8:197. doi: 10.1186/1471-2407-8-197. PMID: 18620555; PMCID: PMC2478682.

Pabla N, Dong Z. Cisplatin nephrotoxicity: mechanisms and renoprotective strategies. Kidney Int. 2008 May;73(9):994-1007. doi: 10.1038/sj.ki.5002786. Epub 2008 Feb 13. PMID: 18272962.

Padilha CS, Borges FH, Costa Mendes da Silva LE, Frajacomo FTT, Jordao AA, Duarte JA, Cecchini R, Guarnier FA, Deminice R. Resistance exercise attenuates skeletal muscle oxidative stress, systemic pro-inflammatory state, and cachexia in Walker-256 tumor-bearing rats. Appl Physiol Nutr Metab. 2017 Sep;42(9):916-923. doi: 10.1139/apnm-2016-0436. Epub 2017 May 5. PMID: 28475846.

Parker WB. Enzymology of purine and pyrimidine antimetabolites used in the treatment of cancer. Chem Rev. 2009 Jul;109(7):2880-93. doi: 10.1021/cr900028p. PMID: 19476376; PMCID: PMC2827868.

Peixoto da Silva, S., Santos, J. M. O., Costa E Silva, M. P., Gil da Costa, R. M., & Medeiros, R. (2020). Cancer cachexia and its pathophysiology: links with sarcopenia, anorexia and asthenia. Journal of cachexia, sarcopenia and muscle, 11(3), 619–635. https://doi.org/10.1002/jcsm.12528

Peng DJ, Wang J, Zhou JY, Wu GS. Role of the Akt/mTOR survival pathway in cisplatin resistance in ovarian cancer cells. Biochem Biophys Res Commun. 2010 Apr 9;394(3):600-5. doi: 10.1016/j.bbrc.2010.03.029. Epub 2010 Mar 7. PMID: 20214883; PMCID: PMC4063277.

Perše M. Cisplatin Mouse Models: Treatment, Toxicity and Translatability. Biomedicines. 2021 Oct 7;9(10):1406. doi: 10.3390/biomedicines9101406. PMID: 34680523; PMCID: PMC8533586.

Petersen AM, Pedersen BK. The role of IL-6 in mediating the anti-inflammatory effects of exercise. J Physiol Pharmacol. 2006 Nov;57 Suppl 10:43-51. PMID: 17242490.

Rius-Pérez S, Torres-Cuevas I, Millán I, Ortega ÁL, Pérez S. PGC-1α, Inflammation, and Oxidative Stress: An Integrative View in Metabolism. Oxid Med Cell Longev. 2020 Mar 9;2020:1452696. doi: 10.1155/2020/1452696. PMID: 32215168; PMCID: PMC7085407.

Rocha CRR, Silva MM, Quinet A, Cabral-Neto JB, Menck CFM. DNA repair pathways and cisplatin resistance: an intimate relationship. Clinics (Sao Paulo). 2018 Sep 6;73(suppl 1):e478s. doi: 10.6061/clinics/2018/e478s. PMID: 30208165; PMCID: PMC6113849.

Rodilla V. Origin and evolution of binucleated cells and binucleated cells with micronuclei in cisplatin-treated CHO cultures. Mutat Res. 1993 Aug;300(3-4):281-91. doi: 10.1016/0165-1218(93)90062-i. PMID: 7687030.

Rosenberg B, VanCamp L, Trosko JE, Mansour VH. Platinum compounds: a new class of potent antitumour agents. Nature. 1969;222(5191):385-386. doi: 10.1038/222385a0. PMID: 5787908.

Sadeghi, M.; Keshavarz-Fathi, M.; Baracos, V.; Arends, J.; Mahmoudi, M.; Rezaei, N. Cancer cachexia: Diagnosis, assessment, and treatment. Crit Rev Oncol Hematol. 2018, 127, 91-104; DOI: 10.1016/j.critrevonc.2018.05.006.

Sakai H, Asami M, Naito H, Kitora S, Suzuki Y, Miyauchi Y, Tachinooka R, Yoshida S, Kon R, Ikarashi N, Chiba Y, Kamei J. Exogenous insulin-like growth factor 1

attenuates cisplatin-induced muscle atrophy in mice. J Cachexia Sarcopenia Muscle. 2021 Dec;12(6):1570-1581. doi: 10.1002/jcsm.12760. Epub 2021 Jul 16. PMID: 34268902; PMCID: PMC8718074.

Schmidt SF, Rohm M, Herzig S, Berriel Diaz M. Cancer Cachexia: More Than Skeletal Muscle Wasting. Trends Cancer. 2018 Dec;4(12):849-860. doi: 10.1016/j.trecan.2018.10.001. Epub 2018 Oct 24. PMID: 30470306.

Shailendra P, Baldock KL, Li LSK, Bennie JA, Boyle T. Resistance Training and Mortality Risk: A Systematic Review and Meta-Analysis. Am J Prev Med. 2022 Aug;63(2):277-285. doi: 10.1016/j.amepre.2022.03.020. Epub 2022 May 20. PMID: 35599175.

Shen DW, Pouliot LM, Hall MD, Gottesman MM. Cisplatin resistance: a cellular self-defense mechanism resulting from multiple epigenetic and genetic changes. Pharmacol Rev. 2012 Jul;64(3):706-21. doi: 10.1124/pr.111.005637. Epub 2012 Jun 1. PMID: 22659329; PMCID: PMC3400836.

Sheth S, Mukherjea D, Rybak LP, Ramkumar V. Mechanisms of Cisplatin-Induced Ototoxicity and Otoprotection. Front Cell Neurosci. 2017 Oct 27;11:338. doi: 10.3389/fncel.2017.00338. PMID: 29163050; PMCID: PMC5663723.

Siddik Z. H. (2003). Cisplatin: mode of cytotoxic action and molecular basis of resistance. Oncogene, 22(47), 7265–7279. https://doi.org/10.1038/sj.onc.1206933.

Siddiqui JA, Pothuraju R, Jain M, Batra SK, Nasser MW. Advances in cancer cachexia: Intersection between affected organs, mediators, and pharmacological interventions. Biochim Biophys Acta Rev Cancer. 2020 Apr;1873(2):188359. doi: 10.1016/j.bbcan.2020.188359. Epub 2020 Mar 25. PMID: 32222610; PMCID: PMC8132467.

Silvennoinen M, Ahtiainen JP, Hulmi JJ, Pekkala S, Taipale RS, Nindl BC, Laine T, Häkkinen K, Selänne H, Kyröläinen H, Kainulainen H. PGC-1 isoforms and their target genes are expressed differently in human skeletal muscle following resistance and endurance exercise. Physiol Rep. 2015 Oct;3(10):e12563. doi: 10.14814/phy2.12563. PMID: 26438733; PMCID: PMC4632948.

Sirago G, Conte E, Fracasso F, Cormio A, Fehrentz JA, Martinez J, Musicco C, Camerino GM, Fonzino A, Rizzi L, Torsello A, Lezza AMS, Liantonio A, Cantatore P, Pesce V. Growth hormone secretagogues hexarelin and JMV2894 protect skeletal muscle from mitochondrial damages in a rat model of cisplatin-induced cachexia. Sci Rep. 2017 Oct 12;7(1):13017. doi: 10.1038/s41598-017-13504-y. PMID: 29026190; PMCID: PMC5638899.

Solheim, T. S.; Laird, B.; Balstad, T. R.; Bye, A.; Stene, G.; Baracos, V.; Strasser, F.; Griffiths, G.; Maddocks, M.; Fallon, M.; et al. Cancer cachexia: rationale for the MENAC (Multimodal-Exercise, Nutrition and Anti-inflammatory medication for Cachexia) trial. BMJ supportive & palliative care. 2018, 8, 258–265; https://doi.org/10.1136/bmjspcare-2017-001440

Sorimachi H, Ono Y. Regulation and physiological roles of the calpain system in muscular disorders. Cardiovasc Res. 2012 Oct 1;96(1):11-22. doi: 10.1093/cvr/cvs157. Epub 2012 Apr 27. PMID: 22542715; PMCID: PMC3444232.

Stanton RA, Gernert KM, Nettles JH, Aneja R. Drugs that target dynamic microtubules: a new molecular perspective. Med Res Rev. 2011 May;31(3):443-81. doi: 10.1002/med.20242. Epub 2011 Mar 4. PMID: 21381049; PMCID: PMC3155728.

Steensberg A, Keller C, Starkie RL, Osada T, Febbraio MA, Pedersen BK. IL-6 and TNF-alpha expression in, and release from, contracting human skeletal muscle. Am J Physiol Endocrinol Metab. 2002 Dec;283(6):E1272-8. doi: 10.1152/ajpendo.00255.2002. Epub 2002 Aug 20. PMID: 12388119.

Tilsed CM, Fisher SA, Nowak AK, Lake RA, Lesterhuis WJ. Cancer chemotherapy: insights into cellular and tumor microenvironmental mechanisms of action. Front Oncol. 2022 Jul 29;12:960317. doi: 10.3389/fonc.2022.960317. PMID: 35965519; PMCID: PMC9372369.

Tisdale MJ. Cachexia in cancer patients. Nat Rev Cancer. 2002 Nov;2(11):862-71. doi: 10.1038/nrc927. PMID: 12415256.

Uciechowski P, Dempke WCM. Interleukin-6: A Masterplayer in the Cytokine Network. Oncology. 2020;98(3):131-137. doi: 10.1159/000505099. Epub 2020 Jan 20. PMID: 31958792.

Von Haehling, S.; Anker, S.D. Cachexia as a major underestimated and unmet medical need: facts and numbers. J Cachexia Sarcopenia Muscle. 2010, 1, 1-5; DOI: 10.1007/s13539-010-0002-6.

Wang, X. L., Wang, L., Lin, F. L., Li, S. S., Lin, T. X., & Jiang, R. W. (2021). Protective Effect of Penetratin Analogue-Tagged SOD1 on Cisplatin-Induced Nephrotoxicity through Inhibiting Oxidative Stress and JNK/p38 MAPK Signaling Pathway. Oxidative medicine and cellular longevity, 2021, 5526053. https://doi.org/10.1155/2021/5526053.

Webster JM, Kempen LJAP, Hardy RS, Langen RCJ. Inflammation and Skeletal Muscle Wasting During Cachexia. Front Physiol. 2020 Nov 19;11:597675. doi: 10.3389/fphys.2020.597675. PMID: 33329046; PMCID: PMC7710765.

Yano S, Zhang Y, Miwa S, Tome Y, Hiroshima Y, Uehara F, Yamamoto M, Suetsugu A, Kishimoto H, Tazawa H, Zhao M, Bouvet M, Fujiwara T, Hoffman RM. Spatial-temporal FUCCI imaging of each cell in a tumor demonstrates locational dependence of cell cycle dynamics and chemoresponsiveness. Cell Cycle. 2014;13(13):2110-9. doi: 10.4161/cc.29156. Epub 2014 May 8. PMID: 24811200; PMCID: PMC4111702.

Yu D, Gu J, Chen Y, Kang W, Wang X, Wu H. Current Strategies to Combat Cisplatin-Induced Ototoxicity. Front Pharmacol. 2020 Jul 3;11:999. doi: 10.3389/fphar.2020.00999. PMID: 32719605; PMCID: PMC7350523.

Yu, W., Chen, Y., Dubrulle, J., Stossi, F., Putluri, V., Sreekumar, A., Putluri, N., Baluya, D., Lai, S. Y., & Sandulache, V. C. (2018). Cisplatin generates oxidative stress which is accompanied by rapid shifts in central carbon metabolism. Scientific reports, 8(1), 4306. https://doi.org/10.1038/s41598-018-22640-y.

Zhang HL, Wang MD, Zhou X, Qin CJ, Fu GB, Tang L, Wu H, Huang S, Zhao LH, Zeng M, Liu J, Cao D, Guo LN, Wang HY, Yan HX, Liu J. Blocking preferential glucose uptake sensitizes liver tumor-initiating cells to glucose restriction and

sorafenib treatment. Cancer Lett. 2017 Mar 1;388:1-11. doi: 10.1016/j.canlet.2016.11.023. Epub 2016 Nov 26. PMID: 27894955.

Zhang L, Wu X, Xu T, Luo C, Qian J, Lu Y. Chemotherapy plus radiotherapy versus radiotherapy alone in patients with anaplastic glioma: a systematic review and meta-analysis. J Cancer Res Clin Oncol. 2013 May;139(5):719-26. doi: 10.1007/s00432-013-1387-3. Epub 2013 Feb 10. PMID: 23397358.